DOKUZ EYLÜL UNIVERSITY

GRADUATE SCHOOL OF NATURAL AND APPLIED SCIENCES

DEVELOPMENT AND CHARACTERIZATION OF CARBON BASED TEMPERATURE SENSORS

by

Özgür Yasin KESKİN

January, 2025

İZMİR

DEVELOPMENT AND CHARACTERIZATION OF CARBON BASED TEMPERATURE SENSORS

A Thesis Submitted to the
Graduate School of Natural and Applied Sciences of Dokuz Eylül University
In Partial Fulfillment of the Requirements for the Degree of Doctor of Philosophy in Department of Metalurgy and Material Engineering,
Metalurgy and Material Engineering Program

by

Özgür Yasin KESKİN

January, 2025

İZMİR

Ph.D. THESIS EXAMINATION RESULT FORM

We have read the thesis entitled **"DEVELOPMENT AND CHARACTERIZATION OF CARBON BASED TEMPERATURE SENSORS"** completed by **ÖZGÜR YASİN KESKİN** under supervision of **PROF.DR. MUSTAFA EROL** and we certify that in our opinion it is fully adequate, in scope and in quality, as a thesis for the degree of Doctor of Philosophy.

Prof. Dr. Mustafa EROL

Supervisor

Prof. Dr. Kadriye ERTEKİN

Thesis Committee Member

Asst. Prof. Dr. Bahadır UYULGAN

Thesis Committee Member

Prof. Dr. Fethullah GÜNEŞ

Examining Committee Member

Assoc. Prof. Dr. Yavuz ÖZTÜRK

Examining Committee Member

Prof. Dr. Abdullah SEÇGİN

Director

Graduate School of Natural and Applied Sciences

ACKNOWLEDGMENT

Firstly, I would like to express my deepest gratitude to my advisor, Prof. Dr. Mustafa EROL for his supervision, support, guidance, and understanding during my thesis. Also, I would like to thank my thesis committee members, Prof. Dr. Kadriye ERTEKİN, and Assist. Prof. Dr. Bahadır UYULGAN for their valuable suggestions, discussions, and contributions.

Also, I would like to thank Dr. Ahmet Çağrı KILINÇ, Dr. Kadir Cihan TEKİN, Dr. Ramazan DALMIŞ, Dr. Serhan KÖKTAŞ, and Erdem Tevfik ÖZDEMİR for their supports and kind friendship.

Finally, I must thank my wife, Merve Sultan KESKİN, for her patience and support during my thesis. Also, I would like to express my special thanks to my family: to my mother, Muazzez KESKİN, to my father, Hüseyin KESKİN, and my sister, Rukiye KESKİN for their support and encouragement.

Özgür Yasin KESKİN

DEVELOPMENT AND CHARACTERIZATION OF CARBON BASED TEMPERATURE SENSORS

ABSTRACT

The use of sensors in everyday activities has significantly impacted individuals' lives. Sensors are used to monitor and detect environmental inputs, such as temperature, humidity, pressure, etc. Temperature sensors are the most fundamental sensors, and different types of materials have been developed for various applications. This thesis aims to develop a new composite material for temperature sensing applications. Within this scope, two carbon-based materials have been used as conductive fillers. Firstly, biochar was obtained from the pyrolysis of barley straw waste to obtain first conductive filler and commercial graphite was employed as second conductive filler. The raw materials and composite films were characterized by using XRD, SEM, FT-IR, Raman spectroscopy, Profilometer, Hall effect, and DTA-TG instruments. Percolation and co-percolation studies were also carried out to investigate the effect of filler concentration and the effect of the combination of two conductive fillers on electrical properties, respectively. On the other hand, the electrical properties and sensor performance of the films were characterized. The performance of sensors was investigated in terms of linearity, long-term stability, repeatability, and response/recovery time. As a result of studies, a new composite material was successfully used in temperature sensor applications. While graphite-based samples performed better on glass substrate, biochar-based samples performed better on PVC substrate. Moreover, the synergetic effect of two conductive fillers positively influenced the overall sensor performance.

Keywords: Temperature sensors, graphite, biochar, percolation, conductive composite.

KARBON ESASLI SICAKLIK SENSÖRLERİNİN GELİŞTİRİLMESİ VE KARAKTERİZASYONU

ÖZ

Sensörlerin günlük faaliyetlerde kullanılması, bireylerin yaşamları üzerinde önemli bir etkiye sahip olmuştur. Sensörler, çevredeki değişiklikleri izlemek ve tespit etmek için kullanılır. Sıcaklık sensörleri en temel sensörlerdir ve farklı uygulama türleri için farklı malzeme türleri geliştirilmiştir. Bu tezin amacı, sıcaklık algılama uygulamaları için yeni bir kompozit malzeme geliştirmektir. Bu kapsamda, iletken dolgu maddesi olarak iki farklı karbon bazlı malzeme kullanılmıştır. İlk olarak, arpa samanı atıklarının pirolizinden elde edilen biyokömür ve ikinci iletken dolgu maddesi olarak ticari grafit kullanılmıştır. Hammaddeler ve kompozit filmler XRD, SEM, Raman spektroskopisi, Fourier dönüşümlü kızılötesi spektroskopisi, Profilometre, Hall etkisi ve DTA-TG cihazları kullanılarak karakterize edilmiştir. Dolgu maddesi konsantrasyonunun ve iki iletken dolgu maddesinin kombinasyonunun elektriksel özellikler üzerindeki etkisini araştırmak için sırasıyla perkolasyon ve ko-perkolasyon çalışmaları da yapılmıştır. Öte yandan, filmlerin elektriksel özellikleri ve sensör performansı karakterize edilmiştir. Sensörlerin performansı doğrusallık, uzun süreli kararlılık, tekrarlanabilirlik ve tepki/iyileşme süresi açısından incelenmiştir. Çalışmalar sonucunda yeni bir kompozit malzeme sıcaklık sensörü uygulamalarında başarıyla kullanıldı. Grafit bazlı örnekler cam substrat üzerinde daha iyi performans sergilerken, biyokömür bazlı örnekler PVC substrat üzerinde daha iyi performans sergilemiştir. Öte yandan, iki iletken dolgu maddesinin sinerjik etkisi genel sensör performansını olumlu yönde etkilemiştir.

Anahtar kelimeler: Sıcaklık sensörleri, grafit, biyokömür, perkolasyon, iletken kompozit.

CONTENTS

Page

LIST OF FIGURES

Page

LIST OF TABLES

Page

CHAPTER ONE
INTRODUCTION

1.1 Background

Incorporating sensor technologies into nearly every aspect of daily life has resulted in numerous benefits for human beings. These technologies have become an indispensable component of contemporary society. (Javaid, Haleem, Rab, et al., 2021). Sensors are defined as devices that monitor, detect, and convert physical changes in the environment into observable electrical signals (Meijer et al., 2014). They enhance the observational capabilities of humans and significantly improve the quality of their lives in all fields. (Vetelino & Reghu, 2017). Pressure, mass flow, temperature, and force sensors are common types of readily available sensors. They are utilized in a diverse range of sectors, including automotive, healthcare, aerospace, and daily living (Bhattacharya et al., 2019; Y. Wang et al., 2022). Furthermore, sensor systems are integral to the production processes of advanced smart factories and automated systems (Javaid, Haleem, Singh, et al., 2021; Kumar, 2018).

One of the most fundamental and critical variables for humans is temperature, which is of vital importance to humans and is usually used as one of the main reference values for identifying health-related problems (Z. Chen et al., 2016). Also, measuring and controlling temperature with high precision and accuracy is essential for efficiency and protection against damage in automation and manufacturing industries (Michalski, 2001).

The most common commercially available temperature sensors are resistance thermometers, thermistors, thermocouples, and infrared thermometers. These types of sensors are generally composed of various metals and semiconductors. The general principle for measurement of temperature in these devices relies on changes in the resistivity of material with temperature. Change in resistance of metal with temperature was first mentioned by Humphry Davy in 1821, and the first commercial

resistive type thermometer was designed by William Siemens in 1871. Due to their simple circuit structure, sensitivity, and long-term stability, they have become the most common temperature sensors today. While commercially available contact-based temperature sensors have high resolution and precision, they cannot be used in every application, such as body monitoring, harsh conditions, complex geometries, etc. (Nag et al., 2022b). As the service requirements vary with different kinds of applications, the required service conditions have not been met by traditional sensors. The increasing demand for sensors in a range of sophisticated applications has prompted the development of composites for sensor applications (Chaudhari, 2020; Matthias Nau, 2002; Meijer et al., 2014).

Temperature-sensitive conductive composites (TSCC) consist of conductive filler and insulating matrix material. Carbon-based materials, conductive polymers, and metallic particles are most commonly used as conductive fillers, while polymers and co-polymers are preferred as matrix materials. The most frequently utilized substrates are composed of ceramics, polymers, textiles, and papers (Arman Kuzubasoglu & Kursun Bahadir, 2020a; Q. Li et al., 2017; Matthias Nau, 2002). Due to their properties, such as lightweightness, flexibility, and cost-effective productibility, TSCCs are considered as alternative materials to conventional rigid materials for sensor applications. A considerable amount of research has been conducted to develop TSCC by incorporating a variety of conductive fillers into a polymer matrix. (Megha et al., 2018; Rahman et al., 2019; Shih et al., 2010). Carbon-based materials are emerging as promising candidates for use as conductive fillers in composites, offering a range of advantageous properties. (Z. Li et al., 2019).

Carbon-based materials show great promise in enhancing conductivity in electrical components, composites, and devices. It is possible that they may improve the overall performance and reliability of electrical applications. Their exceptional properties, including high electrical conductivity, mechanical strength, and thermal stability, distinguish them from other materials utilized as conductive fillers. The chemical stability of the carbon-based materials ensures long-term durability and performance

in various environmental conditions. These materials maintain their conductive properties over an extended period, making them a reliable choice for various applications. The excellent thermal stability of carbon-based materials ensures that they can withstand high temperatures without compromising their conductivity. This makes them suitable for applications that require resistance to heat and thermal stress (Jariwala et al., 2013).

As research in this field continues to progress, scientists and engineers are exploring new ways to enhance the performance and functionality of TSCCs with novel materials and manufacturing techniques (S. Khan et al., 2023). The objective is to develop composite materials that can change their conductivity in response to temperature fluctuations, thereby creating a vast array of potential applications across diverse industries. Recently, carbon-based conductive fillers have been used to make conductive composites due to advantages such as giving opportunity for flexibility, high conductivity, and chemical stability, etc. (Huang et al., 2019; Q. Liu et al., 2019; Tonkov et al., 2022; Wu et al., 2019; Yurddaskal et al., 2017). In this context, sodium silicate solution and biochar/graphite were employed as innovative matrix materials and fillers, respectively. The sensor performance of composites was investigated under heating. This ongoing innovation holds great promise for the future of materials science and technology, paving the way for the creation of advanced materials that can adapt and respond to changing environmental conditions.

1.2 Organization of Thesis

The aim of this thesis is to prepare, characterize, and develop a new composite material for temperature sensing applications. Sodium silicate solution and two distinct conductive carbon-based materials were employed as the fillers and matrix material, respectively. The temperature response of graphite and biochar and their synergistic effect were investigated.

Chapter 2 provides a theoretical background of the temperature sensor technology. The working principles, types of temperature sensors, and their materials were presented in the second chapter. It also summarizes carbon-based materials and related recent studies. Chapter 3 provides information on experimental studies. The fabrication and characterization of the sensors were given in detail. Chapter 4 covers the characterization results of raw and composite materials, sensor performance results, and discussions on the overall results of the studies. Finally, the general conclusions of the study and future plans are given in Chapter 5.

CHAPTER TWO
THEORETICAL BACKGROUND

2.1 Temperature Sensors

Temperature sensors are devices that can detect the degree of hotness or coolness in an object and convert it into meaningful data for humans. When the kinetic energy of atoms increases during heating, they can transfer it to their surroundings until they become thermodynamically equal in temperature. The transferred energy is referred to as “heat,” and the change in kinetic energy of atoms can change the physical condition of materials, such as volumetric expansion, increase or decrease in resistance, and vapor pressure. The device that measures such physical changes as a function of temperature forms the basis of temperature sensors (Fraden, 2010). The most prevalent temperature sensors in commercial applications are thermocouples, thermistors, and resistance temperature detectors. They are the most common sensors for industry and daily life (Vetelino & Reghu, 2017).

2.1.1 Thermocouples

Thermocouples are the most utilized type of temperature sensor, primarily due to their extensive temperature range applicability, low cost, and straightforward operational characteristics. Thermocouples are comprised of two distinct electric conductors joined at one end (Figure 2.1). This connection point, known as a "junction," enables the generation of voltage or potential difference in accordance with temperature fluctuations (Matthias Nau, 2002). This physical phenomenon was discovered by Johann Seebeck and is called the Seebeck effect or thermoelectric effect. According to Seebeck's theory, the flow of heat through a conductor gives rise to a net movement of electrons from the region of higher temperature to that of lower temperature. This phenomenon is known as electromotive force (EMF) (Ravindra et al., 2018). Thanks to the Seebeck effect, the temperature can be determined by measuring the amount of electricity generated. In summary, a thermocouple is a device that facilitates the conversion of thermal energy into electrical energy.

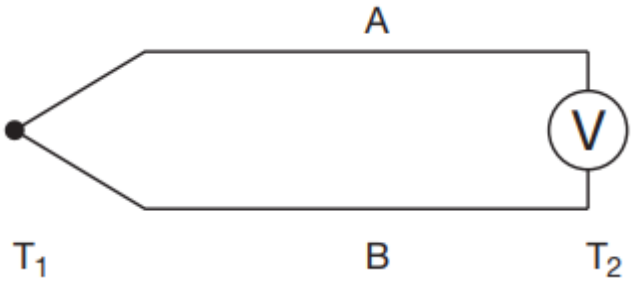

Figure 2.1 Basic schematic of a thermocouple

2.1.2 Thermistors

The term "thermistors," which combines the terms "therm" (thermal) and "resistor" (resistance), refers to substances whose resistance varies with temperature. The defining feature of a thermistor, a thermally sensitive resistor, is its ability to alter its electrical resistance in response to changes in temperature. Thermistors can be classified in accordance with the temperature coefficient, as either negative temperature coefficient (NTC) or positive temperature coefficient (PTC) devices, depending on the changes in the sensor material's resistance against temperature change (Figure 2.2) (Webster & Eren, 2018).

Metals, including iron, titanium, chromium, manganese, copper, and cobalt, are used to make NTC thermistors. When the temperature rises, these devices show a monotonic decrease in electric resistance. NTC thermistors generally have non-linear characteristics, and due to these characteristics, the sensitivity of sensors varies with temperature. Despite the inherent non-linearity of NTC thermistors, it is possible to achieve good linearity by using a thermistor-resistor network or incorporating innovative materials (Macklen, 1991).

PTC thermistors can be classified into two distinct categories: silicon-based PTC thermistors and switching-type PTC thermistors. Silicon-based thermistors have nearly linear behavior and resistance-temperature characteristics related to the bulk properties of silicon. They have a sensitivity of 0.7 to 0.8 % $°C^{-1}$. The second type of

thermistors is switching-type PTC thermistors. The composition of these materials is a mixture of lead, barium, and strontium titanates. While they show NTC characteristics at low temperatures, they exhibit PTC characteristics with increasing temperatures (Rajanna, K., Nayak, 2004). The temperature at which the switching occurs for this particular thermistor varies between 80 and 240℃, and after this switching temperature, the PTC characteristic becomes dominant (Webster & Eren, 2018).

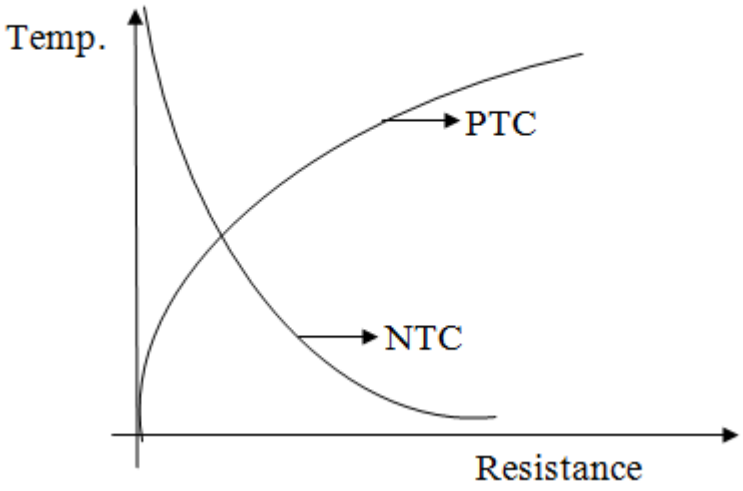

Figure 2.2 Representation of NTC and PTC behavior as a function of temperature

2.1.3 Resistance Temperature Detectors (RTD)

Resistance Temperature Detectors (RTDs) are a typical tool used for temperature measurement. The temperature measurements with these electrical temperature meters are more accurate than other counterparts. It is established that specific metals exhibit a predictable alteration in their electric resistance in response to temperature changes. The metal's electrical resistance rises with temperature, and electric resistance drops with decreasing temperatures. This feature is the main principle for temperature measurement via RTDs (Webster & Eren, 2018).

The mobility of the conduction electrons or electron cloud determines a metal's electrical conductivity. The electrons in a metal flow toward the positive pole when a voltage is applied. Imperfections in the crystalline structure of metals impede mobility; this impediment is defined as resistance. Grain boundaries, dislocations, and absent lattice atoms are examples of some defects in the crystal structure. Dislocations cause a constant resistance because they are not temperature-dependent phenomena. The mobility of the conducting electrons is restricted by the metal lattice's atoms which oscillate more due to increasing temperature. As the oscillation of atoms increases, the linear resistance of the system increases. By measuring the resistance of the material, the temperature can be calculated by mathematical approximations (Leigh, 1988).

In the case of metal-based transducers, the most commonly utilized metals are copper, nickel, and platinum, which are typically employed as sensing materials for RTDs. Copper is typically utilized within a temperature range of -100°C to 100°C, offering a cost-effective solution. In addition, Nickel and its alloys are used due to their higher resistivity and temperature coefficients of resistance (TCR). However, they exhibit non-linear and strain-sensitive fluctuation in electrical resistance with temperature. Due to its higher melting point (around 1769°C), corrosion resistance, and a well-established temperature coefficient of resistance, Platinum is a popular choice for accurate temperature measurements between –260°C and 1000°C. Although platinum is not the most sensitive metal, its long-term stability makes it the most widely utilized material for developing RTDs. (Childs, 2001).

2.2 Conductive Materials for Temperature Sensors

The most important component of a temperature sensor is the material that is responsible for detecting temperature changes. Various materials have been used based on the mechanism and temperature range of the sensor to accurately sense temperature fluctuations (Y. Su et al., 2020). As aforementioned, pure metals are the most frequently utilized materials that are sensitive to temperature changes. These materials include platinum (Pt) (Y. Su et al., 2020), nickel (Ni) (Lichtenwalner et al., 2007), copper (Cu) (Husain & Kennon, 2013), gold (Au) (Hammock et al., 2013), and

aluminum (Al) (Yoon et al., 2016) in various forms such as films or wires. In addition, other commonly used temperature-sensitive materials are liquid metals and semiconductors (Aslinezhad, 2020; Q. Wang et al., 2015).

On the other hand, various other materials can exhibit electrical conductivity, such as thermo-sensitive polymer conductive pastes, temperature-sensitive conductive composites (TCSS), and conductive polymer-based materials (Phadkule & Sarma, 2023a). Recently, there has been a great deal of research into the development of conductive composites with carbon-based additives which are sensitive to temperature changes (Nag et al., 2022a; Turkani et al., 2018; N. Wang et al., 2022a). These materials are graphene, graphene oxide (GO), reduced graphene oxide (rGO), graphite, and carbon nanotubes (CNTs), which are highly versatile and provide significant advantages and unique properties when incorporated into the matrix material. In particular, their excellent conductivity, heat resistance, strength, and chemical stability make them essential components in the field of sensor design and development (C. Wang et al., 2019). Incorporating carbonaceous materials into sensors improves overall functionality and ensures accurate and precise detection of various stimuli (Choi et al., 2016; Y. Khan et al., 2016). Their ability to conduct electricity and withstand high temperatures makes them suitable for sensor applications in demanding environments. Furthermore, these materials offer resistance to corrosion and degradation, ensuring the longevity and endurance of the sensors. Also, giving the opportunity to use the flexible matrix make them attractive materials for sensor applications where harmonic and flexible applications are required (C. Wang et al., 2019).

2.2.1 Carbon-based materials

Carbon is an essential structural component of all living beings and is among the most pervasive elements on Earth. Furthermore, carbon is distinctive in that it is the sole element within the periodic table that can exist in various allotropic forms, encompassing structures from zero-dimensional to three-dimensional., resulting from its versatile hybridization abilities.

Carbon can exist in both crystalline and amorphous structures (Inagaki & Kang, 2016). The term "crystalline form of carbon" is used to describe the ordered and regular arrangement of carbon atoms within a material. In contrast, the amorphous form of carbon lacks a defined structure and is characterized by a higher degree of disorder. The two forms of carbon exhibit distinctive properties and are applicable in various scientific and technological disciplines. The crystalline forms of carbon are fullerene, diamond, and graphite, which exhibit strong and consistent bonding between their atoms, giving rise to hardness and conductivity. On the other hand, the amorphous forms of carbon, coal, charcoal, and lamp black possess a more random arrangement of atoms, resulting in their diverse properties and flexibility in different environments (Mathur, 2016). Understanding the differences between these two forms of carbon is crucial for researchers and engineers to harness their distinct characteristics for specific purposes. Moreover, the groundbreaking discoveries and advancements in different forms of carbon (graphene, carbon nanotube) have unlocked numerous possibilities for developing innovative materials and Technologies (Dai, 2006). The most widely used carbon-based materials for sensor applications are graphene, GO, CNT, graphite, and carbon black. Recently, biomass-derived carbon materials also have been getting attention due to their abundance, sustainability, giving the ability to modification of properties (Malode et al., 2023; Tiwari et al., 2022; L. Wang et al., 2014).

2.2.1.1 Graphite

One alternative hybridization pattern for the bonding electrons is possible when the carbon atoms form hexagonal rings. Each layer, known as a graphene sheet, is indeed a molecule with stable covalent bonds (Mathur, 2016). Graphite exhibits anisotropic properties, exhibiting superior electrical and thermal conductivity in the direction parallel to its graphene layers. This is attributed to the delocalized electrons within the layers, which facilitate the movement of electrons. However, the conductivity perpendicular to the layers is poor due to the weak van der Waals interactions between layers. The electrical conductivity of graphite allows it to be utilized as

electrochemical electrodes and electric brushes. Due to its anisotropic nature, the layers of carbon in graphite can readily slide against each other, making it an effective lubricant and material for pencils (Chung, 2002).

The atomic structure of graphite is composed of layers, wherein the atoms are arranged in a hexagonal configuration. (Figure 2.3). These layers are arranged in a specific sequence known as the AB sequence. The hexagonal unit cell of graphite consists of a layered structure with lattice spacing between two identical sheets with c:6.70 Å, and a:2.46 Å. Also, the distance between the two adjacent layers is d = 3.35 Å (Mathur, 2016).

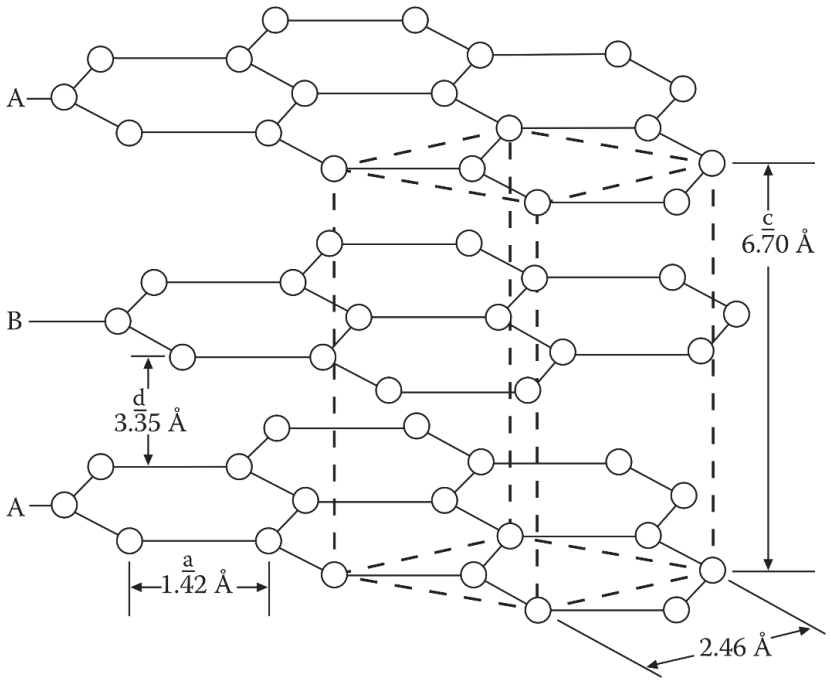

Figure 2.3 Crystal structure of Graphite (Mathur, 2016)

The layer structure of graphite provides unique properties and characteristics essential for its various applications. This distinct layer structure influences its

conductivity, thermal conductivity, mechanical strength, and lubricating properties. Graphite's versatility and usefulness in a diverse range of fields can be attributed to its specific layer arrangement, making it a valuable material for numerous applications (Mathur, 2016).

2.2.1.2 Graphene and Graphene Oxide

Graphene is the fundamental component of a range of carbon-based substances. It is a crystalline material comprising just one atom thick, arranged in a two-dimensional lattice structure. It is the main component of all other graphitic forms of carbon, such as (0D) fullerenes, one-dimensional (1D) carbon nanotubes, and three-dimensional (3D) graphite (Figure 2.4) (Mathur, 2016; Saba et al., 2019).

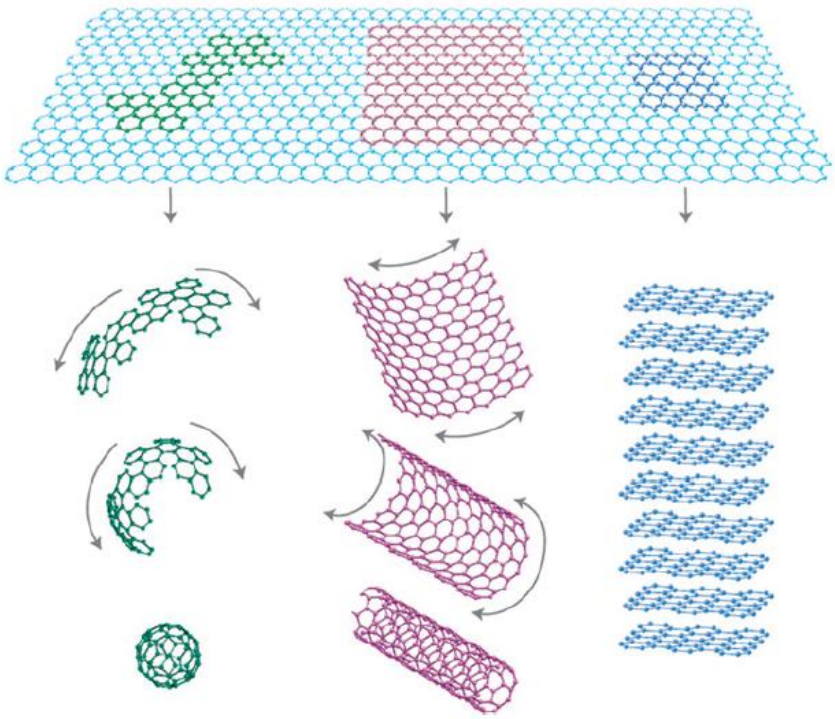

Figure 2.4 Graphene and other graphitic carbon derivatives (Geim & Novoselov, 2009)

The distinctive lattice structure of graphene endows it with remarkable mechanical strength and flexibility, enabling its utilization in many applications. Graphene's remarkable properties stem from the 2p orbitals creating bands known as π states that

spread out across the carbon sheet, making up graphene. The distinctive characteristics of graphene, including its high electrical and thermal conductivity, have generated considerable interest within the scientific community with regard to its potential utilization in a range of advanced technological applications, such as electronics, energy storage, and medical devices. The unique structure of graphene allows for maximum electron mobility, making it an ideal material for high-performance electronic devices. Its exceptional thermal conductivity also makes it promising for heat dissipation and thermal management systems applications. The remarkable mechanical properties of graphene, including high tensile strength and flexibility, open up possibilities for developing advanced composites and materials with superior performance characteristics. The ultrathin nature of graphene provides an attractive basis for developing flexible and transparent electronic devices, including touchscreens and wearable sensors. (Geim & Novoselov, 2009; Rao et al., 2009).

Various techniques can be employed to synthesize graphene, affording a wide range of possibilities for production. These methods include chemical vapor deposition (CVD), which comprises the deposition of carbon atoms onto a substrate within a controlled environment. (Chae et al., 2009). Another method is chemical exfoliation, where graphene is obtained by exfoliating graphite using chemical processes (Parvez et al., 2015). Mechanical exfoliation of graphite is another technique where graphene layers are separated from graphite by physically peeling them off (Fukada et al., 2012). Epitaxial growth is a method where graphene is grown on a crystal substrate, allowing for high-quality graphene to be produced (Tetlow et al., 2014). Reduction of graphite oxide involves the reduction of graphene oxide to graphene through chemical and thermal processes (Pei & Cheng, 2012). Unzipping carbon nanotubes (CNTs) is a method in which graphene is obtained by unzipping carbon nanotubes, resulting in graphene nanoribbons (Y. S. Li et al., 2016). Pyrolysis is a technique where graphene is produced by heating carbon-containing precursors in an inert atmosphere (Amirov et al., 2015). Successive intercalation involves the intercalation of graphite layers with guest molecules, leading to the formation of graphene. Grafting is a method where functional groups are attached to graphite, allowing for the synthesis of functionalized graphene. Self-exfoliation of graphite oxide is a technique where graphene oxide is

exfoliated to obtain graphene (L. Chen et al., 2012). Each of these methods provides a distinctive approach to synthesizing graphene, offering researchers a diverse range of options to select from in accordance with their particular requirements and objectives.

The utilization of graphite oxide as a precursor has facilitated the exploration of novel avenues for the advancement and large-scale manufacturing of graphene-based materials. Graphite oxide is regarded as a promising initial material for the cost-effective and efficient production of graphene-based materials on a large scale. One of the most commonly employed techniques for the synthesis of graphene is the exfoliation of graphite oxide in a liquid phase. The process entails the treatment of graphite powder with potent oxidizing agents to generate graphite oxide, which is then subjected to sonication to expand and exfoliate the oxidized layers. This results in the separation of the layers of graphite oxide, forming thin sheets of graphene. This approach enables the fabrication of superior-quality graphene at a reduced cost. Liquid-phase exfoliation is particularly favored for its simplicity and scalability in producing graphene from graphite oxide. By using graphite oxide as a precursor, researchers and manufacturers can optimize production processes and reduce costs associated with graphene production. The liquid-phase exfoliation method offers a versatile and efficient way to obtain graphene from graphite oxide with less complexity and resource consumption. This approach enables the fabrication of graphene in diverse forms and dimensions, rendering it a promising candidate for various applications across diverse sectors, including electronics, energy storage, and biomedical engineering. (Dimiev & Eigler, 2016).

2.2.1.3 Carbon Nanotube

Carbon nanotubes (CNTs) are unique nanomaterials with cylindrical structures with hollow interiors. The structures in consideration are constituted by carbon atoms that are arranged in a network of hexagons on the surface. The bonding between these carbon atoms in CNTs is characterized by sp^2 hybridization, which is the same bonding pattern found in graphite (Georgakilas et al., 2015). Although carbon nanotubes are produced by rolling graphene sheets, it is crucial to acknowledge that these two

materials exhibit distinctive properties that differentiate them from one another. For instance, properties such as electrical conductivity and mechanical strength also vary between the two materials due to their different structures and compositions (Ando, 2009; Papageorgiou et al., 2017). Two principal categories of carbon nanotubes are distinguished: single-walled (SWCNTs) and multi-walled (MWCNTs) (see Figure 2.5). Single-walled carbon nanotubes (SWCNTs) are formed by wrapping a single layer of graphene sheets around a central core of carbon atoms, resulting in a hollow cylindrical structure. Multi-walled carbon nanotubes (MWCNTs) are produced through a process of repeated rolling of graphene sheets or a single layer of graphite into cylinders within each other. The diameter of these nanotubes is typically greater than 100 nanometers. (Karimi et al., 2015; Malhotra et al., 2015).

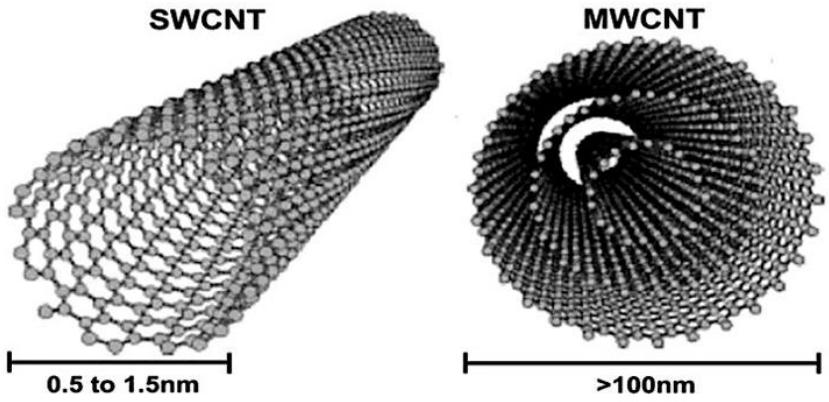

(a) (b)

Figure 2.5 (a) Single walled carbon nanotube (SWCNT) and (b) Multi walled carbon nanotube (MWCNT) (Ribeiro et al., 2017)

CNTs display remarkable properties, including exceptional tensile strength, a vast surface area ranging from 50 to 1315 m^2/g, superior electrical conductivity, and an aspect ratio exceeding 1000. These properties render CNTs highly attractive for utilization in a variety of applications within the fields of nanotechnology and materials science. The outstanding tensile strength of CNTs enables them to withstand high levels of mechanical stress, making them ideal for use in structural materials and

composites that require exceptional durability. Additionally, the large surface area of CNTs allows for increased interactions with surrounding molecules, making them suitable for adsorption, catalysis, and sensing applications. The high electrical conductivity of CNTs makes them valuable for use in electronics, such as in conductive inks, sensors, and energy storage devices. The considerable aspect ratio of CNTs is a key factor in determining their distinctive properties, including their exceptional mechanical properties and high thermal conductivity. These characteristics render CNTs highly versatile materials with a variety of potential applications across numerous industrial sectors. (Aqel et al., 2012; Peigney et al., 2001; Yee et al., 2019).

2.2.1.4 Carbon Black

Carbon black is a form of carbon commonly found in powder form, consisting of tiny spherical particles. These particles have a surface area exceeding 1000 square meters per gram, a particle size smaller than 50 nanometers, and a density lower than 2.25 grams per cubic centimeter, which is the expected density for graphite (Besenhard, 2007). These particles are produced on a large scale through the process of vapor phase pyrolysis and controlled partial combustion of heavy hydrocarbons in gaseous or liquid form (Uddin et al., 2017). It is widely utilized in various commercial and consumer goods, including automotive components, tire manufacturing, colorants, synthetic materials, energy storage devices, and sensing technology (Long et al., 2013). In the industry, carbon black can be produced through four main manufacturing processes. It can be made by oil and gas furnace processes, and thermal and channel processes. Among these, the furnace process is the most widely utilized method for creating tiny particles of carbon black. In this process, heavy fuel or coal oil is introduced into a hot gas stream for incomplete combustion. The gases produced in the furnace reactor, such as carbon monoxide and hydrogen, can be used to generate heat or electricity. This particular process is well suited to high-volume production because of its ability to achieve high yields and effectively control particle size. (Drogin, 1968; Kühner & Voll, 2018).

2.2.1.5 Biochars

Population growth, advances in technology, and the trend towards commercialization have all significantly contributed to increasing the need for fossil fuels. This surge in demand has led to more fossil fuel use, resulting in higher levels of pollution and greenhouse gas emissions that harm the environment. Fossil fuels, which are a finite resource and require millions of years to form, are being rapidly depleted due to human societies' constant reliance on them worldwide. This overconsumption of fossil fuels has caused a gap to develop between the demand for these resources and the available supply, especially within a global expanding economy. Consequently, this situation is predicted to lead to an increase in the price of products derived from fossil fuels in the near future. (Lead et al., 2001).

The overconsumption of products made from fossil fuels has resulted in a dual problem characterized by the depletion of petroleum-based resources and the accumulation of synthetic materials in the environment and food chain. These synthetic materials, primarily composed of polymers, play a significant role in contributing to environmental degradation through their manufacturing, usage, and disposal, ultimately leading to pollution by introducing non-biodegradable substances into the soil and toxic emissions into the atmosphere. The heavy reliance on fossil fuels for materials, goods, and procedures hinders the progress towards building a sustainable future (John & Thomas, 2008).

Two key influences on advancing cutting-edge materials and products are renewability and versatility. As the amount of waste, pollution, and greenhouse gases continues to rise, increasing attention is being paid to creating materials that not only come from waste sources but are also capable of being renewed naturally. Within this framework, biochars are a great candidate as an alternative to other carbon derivatives (Bahari & Krause, 2016). Biochar is the residue that is left behind as a solid product following the process of biomass pyrolysis. Biomass pyrolysis involves subjecting the biological material to elevated temperatures in the complete absence of oxygen, resulting in its thermochemical decomposition. This results in the creation of biochar,

a carbon-rich material with various potential applications (Lehmann & Stephen, 2015). One of the most remarkable advantages of biochar is its ability to be customized in terms of various properties such as surface area, porosity, surface charge, and elemental content. This feature allows biochar to exhibit exceptional performance across a wide range of research fields, including energy materials and environmental remediation (Fan et al., 2018; Qin et al., 2020). Biochar is a substance rich in carbon that shows promise in boosting the strength and heat-resistant qualities of polymers when used as a filler. This natural material has the ability to improve the general performance of polymer-based products through the enhancement of their mechanical properties. In addition to increasing durability, biochar can be used to improve the thermal strength of polymers, making them more suitable for applications that require high temperatures (Adeniyi et al., 2023; Petousis et al., 2024; Velmurugan G et al., 2024).

Incorporating biochar into polymer formulations can help reduce the reliance on traditional fillers that may be harmful to the environment. Incorporating biochar into polymer composites can help improve the overall performance and longevity of the resulting products. Manufacturers can create more environmentally friendly and sustainable products by using biochar as a filler (Rajendran, Palani, Arunprasath, et al., 2024; Rajendran, Palani, Shanmugam, et al., 2024; Rajendran, Palani, Veerasimman, et al., 2024).

2.3 Carbon-based conductive composites

Conductive composites are materials that can detect temperature changes through variations in resistance. They are gaining significant interest due to their properties, such as sensitivity, lightweight nature, flexibility, and cost-effective manufacturing process (Takei et al., 2015; Yang et al., 2015; Yokotaa et al., 2015). They generally consist of conductive fillers in the polymer matrix. This kind of composite typically exhibits ohmic-contact electrical behavior. The conductive composites can show linear or nonlinear resistivity behavior as the temperature increases. The gradient of the

curves is related to the sensitivity of the sensor and the temperature coefficient of resistance (TCR), described by the following equation:

$$TCR\ (\alpha) = \frac{\Delta R/R_0}{\Delta T}\ x\ 100$$

where $\Delta R = R\text{-}R_0$, R, and R_0 are the resistance of the composite at any temperature and initial temperature, respectively. ΔT is a deviation in temperature with time (N. Wang et al., 2022b).

The temperature-sensitive conductive composite consists of a complex network of conductive pathways created by conductive fillers dispersed throughout a matrix. The conductivity of this network depends mainly on the amount of conductive fillers present and its distribution in the matrix (N. Wang et al., 2022b). As filler concentrations increase, the particles begin to contact each other and establish a conductive network in the composite. The electrical conductivity of the structure can rise sharply at a critical filler concentration. (Figure 2.6). This critical point is called the percolation threshold and shows the insulator-to-conductor transition point in terms of conductivity (McLachlan et al., 1990).

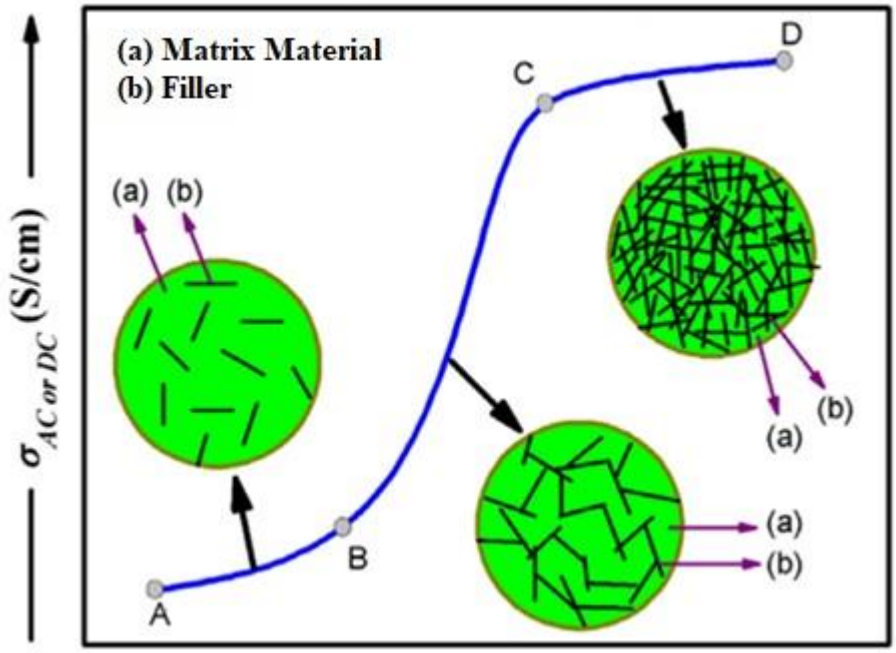

Figure 2.6 Shematic illustraiton of percolaiton theory (Ram et al., 2017)

The electrical behaviors of conductive composites are greatly influenced by changes in temperature. The change in resistivity is primarily due to the mismatch between the thermal expansion coefficients of the filler and the matrix material. As the temperature increases, the distance between two adjacent particles increases, and this causes a rise in the resistance of the composite (Király & Ronkay, 2015). Also, the shape, size, and concentration of filler can affect the resistance of the composite structure (Nagata et al., 1998).

Much research has focused on developing temperature-sensitive conductive composite materials, which involve integrating various types of conductive fillers like carbonaceous materials, electrically conductive polymers, and metallic particles into compatible and insulating polymer matrices. These materials are frequently employed as fillers due to their exceptional properties. Carbon-based materials such as carbon nanotubes (CNT), graphene, carbon black (CB), and graphite are frequently used as conductive fillers due to their remarkable electronic and mechanical characteristics and chemical stability. These materials have unique properties that make them ideal for enhancing the conductivity and overall performance of various composites. Some of the carbon-based temperature-sensitive conductive composites studies are listed in Table 2.1.

Table 2.1 Recent studies about Carbon-based temperature sensors.

Conductive Material	**Matrix Material or Substrate**	**Measurement Range (°C)**	**TCR ($°C^{-1}$)**	**Reference**
Graphite	PDMS	30-110	0.042 (for 25 wt.%)	(Shih et al., 2010)
rGO	PU	30-80	0.0134	(Trung et al., 2016)

Table 2.1 continued

CNT	Polymer tape	20-70	-0.0126	(Karimov et al., 2012)
GO	PEDOT:PSS	25-100	0.0109	(Soni et al., 2020)
rGO	PET	30-100	0.006345	(G. Liu et al., 2018)
Activated Carbon	PET	35-50	-	(D. Liu et al., 2023)
CB	PVC	25-45	0.00148 (for 6 wt.%)	(Xiao et al., 2021)
CB	Kapton tape	28-50	0.00375	(Ali et al., 2019)
Graphene	P(VDF-TrFE)	-20-300	0.025	(Mahmoud & Al-Bluwi, 2020)
CNT	Epoxy	25-160	-	(Neitzert et al., 2011)
CNT	TPU	30-100	-	(G. Zhu et al., 2022)
SWCNT	SEBS	16-55	0.0145	(C. Zhu et al., 2018)
GNWs	PDMS	40-120	0.214	(Yang et al., 2015)
rGO	PHB	20-70	0.008	(Dan & Elias, 2020)

Table 2.1 continued

CNT	XSBR	30-100	0.01636	(Lin et al., 2022)
Graphite	SS solution	25-100	-0.0479 (for 15 wt. %)	(Ozgur Yasin Keskin & Erol, 2023a) (Current Study)

This study represents the production, characterization, and application of Graphite-Biochar/Sodium Silicate solution (SS solution) composite temperature sensors. SS solution was used as matrix material distinctly from the literature. Graphite and biochar were used as conductive materials. Sensor performance of Graphite/SS, Biochar/SS, and Graphite-biochar/SS composites was investigated between 25-100 °C.

2.3.1 Sodium Silicate Solution

Sodium silicate solution ($Na_2.SiO_3.xH_2O$), also known as water-glass, sodium metasilicate, soluble glass, silicate of soda, or liquid glass, is a liquid substance that contains dissolved glass and possesses characteristics similar to water. It consists of anionic silicate, sodium cations, and water (Figure 2.7). These solutions are derived from mineral resources and are considered essential chemicals because of their outstanding properties, such as strong adhesion, ability to form films, cost-effectiveness, and versatility. They serve as a standard example of inorganic polymer mixtures with both electrolyte and polymer properties, acting as an electrolyte solution (Matinfar & Nychka, 2023; Yang, X., Zhu, W., & Yang, 2008).

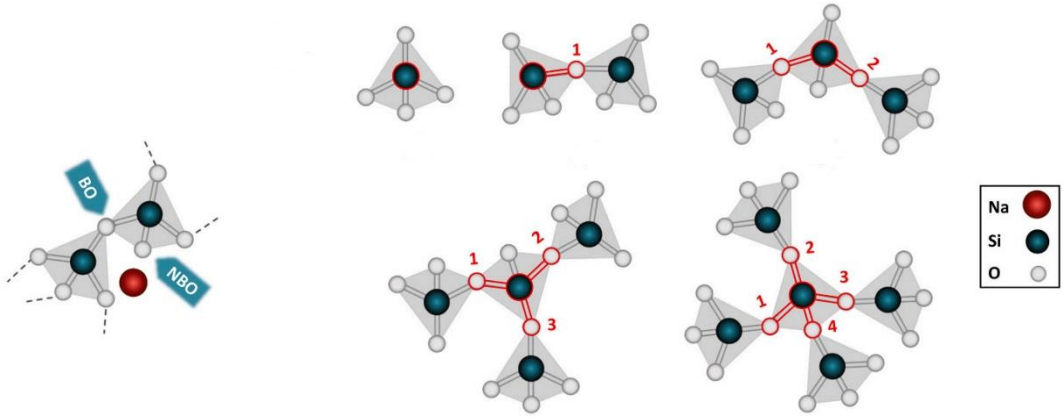

Figure 2.7 Schematic representation of Sodium Silicate structure (Matinfar & Nychka, 2023)

It typically appears as white or gray-white lumps or powder when dry and easily dissolves in water and alkalies but remains insoluble in alcohol and acids. Its versatility and solubility make it a popular choice in various industrial applications and processes. They are widely used as sealants, binders, deflocculants, emulsifiers, and buffers in various industries such as abrasives, casting, construction, and silicate production. These sodium silicate solutions play a vital role in improving the performance and efficiency of many processes in these industries (Owusu, 1982).

CHAPTER THREE
EXPERIMENTAL PROCEDURE

3.1 Materials

In this study, graphite and biochar were used as conductive material, and SS solution was used as matrix material. Graphite powder was purchased from Grapheneexpress. Biomass wastes were obtained from local barley producers to produce biochar, and SS solution was purchased from REFSAN. Glass and Polyvinyl Chloride (PVC) were used as substrate.

3.2 Methods

3.2.1 Production of Biochars

Biomass waste carbon materials were produced with pyrolysis of biomass waste. The production steps of biochars are given in Figure 3.1.

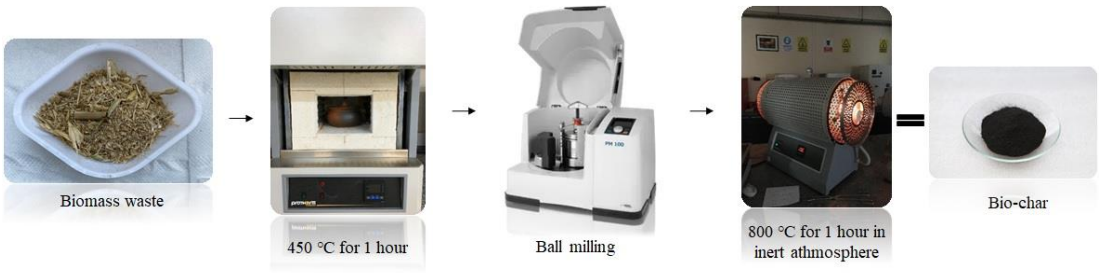

Figure 3.1 Production steps of biochar

Initially, biomass waste was placed in a stew and partially oxidized in an oven at 450°C for one hour. The resulting biochars were subjected to ball milling in order to reduce their size and subsequently pyrolyzed in an oven under inert conditions for one hour at 800°C, to increase the crystallinity of the biochar.

3.2.2 Preparation of Coatings

Commercial Graphite (Gr) and produced biochar (Bc) powders and their combinations with SS solution matrix material were used to develop temperature sensors. Sample abbreviations and ratios are listed in Table 3.1. To determine electrical conductivity percolation thresholds, 1-15, 20, 25, 30 wt.% graphite and 5, 10, 15, 16, 17, 18, 19, 20, 25, 30 wt.% biochar filled composites coating mixture were separately prepared in beakers. The mixtures were then stirred with a magnetic stirrer for 1 hour at room temperature. Subsequently, the beakers were kept immersed in an ultrasonic bath for 30 minutes to obtain more homogenous filler distribution. The samples were abbreviated as XGr (X: 10-20%, Gr:graphite), YBc (Y:20-30%, Bc:biochar), and XGr-YBc (for combination of graphite and biochar).

Table 3.1 Sample abbreviations and definitions

Filler	Concentration (wt %)	Sample name
Graphite	10	10Gr
	15	15Gr
	20	20Gr
Biochar	20	20Bc
	25	25Bc
	30	30Bc
Graphite – Biochar composite	5-1	5Gr-1Bc

Glass and PVC were used as substrates. The preparations were applied to the substrates using the doctor blade technique. The area of the coatings was fixed at 1 x 0.5 cm^2. The deposition was performed and dried at room temperature for 2 hours. The

contact wires were affixed to the coatings via the aforementioned mixture and dried in an oven at 120 ℃ for 12 h.

3.3 Characterization of Filler and Composites

3.3.1 X-Ray Diffractometer (XRD)

X-ray diffraction (XRD) is a fundamental method used to study various types of materials, including powders and crystals. This analytical technique is crucial in determining the crystalline structure and structural phases present in a material. The data obtained from XRD analysis offers valuable insights into the atomic arrangement, crystallinity, and phases of a given substance. The diffraction patterns produced by X-rays interacting with a material can reveal details about the spacing of atoms within the crystal lattice. By analyzing these patterns, researchers can identify the specific crystal structure of a material and the orientation of its crystalline grains (Epp, 2016). The phase analyses of biochar, graphite powder, and powdered SS solution were conducted by using a Rigaku D/Max-2200/PC X-ray diffractometer device with Cu-K_α radiation in the range of 3-90° at 40kV and 30mA.

3.3.2 Raman Spectroscopy

Raman spectroscopy refers to the phenomenon of inelastic scattering of light when interacting with matter. This technique involves measuring the scattered light due to the molecular vibrations in the sample. In Raman spectroscopy, the incident light interacts with the sample, causing photons to gain or lose energy and resulting in a shift in wavelength. This shift in wavelength can provide valuable information about the chemical composition and structure of the material being analyzed.

Raman spectroscopy is a powerful analytical technique that is particularly sensitive to deviations from translational symmetry in a material. It is most effective in detecting covalent bonds that exhibit high levels of symmetry and have minimal or no natural dipole moments. These types of bonds, such as carbon-carbon bonds, perfectly meet

these criteria, making Raman spectroscopy a valuable tool for studying materials composed of these bonds. This spectroscopic method can reveal a wealth of detailed information about the structure of such materials, allowing for comprehensive analysis and investigation (Yang, X., Zhu, W., & Yang, 2008). Raman spectra of the samples were obtained utilising a Raman system with a wavelength of 532 nm (Renishaw Raman Spectrometer).

3.3.3 Fourier Transform Infrared Spectroscopy (FT-IR)

Fourier transform infrared (FT-IR) spectroscopy is a highly effective technique for identifying the types of chemical bonds present in a molecule. This is achieved by producing an infrared absorption spectrum, which can be considered a molecular "fingerprint". Therefore, infrared spectroscopy can result in qualitative analysis of every different kind of material. The interpretation of the infrared absorption spectrum allows for the determination of the chemical bonds present within a molecule. The vibrational frequencies of molecular bonds are dependent upon the elements and the type of bond involved. In the case of an individual bond, a number of specific frequencies have been identified at which it is capable of vibrating. The absorption of light energy results in the excitation of the bond, which in turn increases the frequency of molecular vibration. In general, the lowest frequency is associated with the ground state, while higher frequencies are linked to the excited states. The energy differential between the two states is directly proportional to the light energy, which is, in turn, dependent on the wavelength of the light. Especially the FT-IR method is well-suited for organic materials. The spectroscopic analysis of the barley straw and SS solution was conducted using a Perkin Elmer Spectrum BX instrument equipped with an attenuated total reflection (ATR) apparatus within the spectral range of 4000 to 650 cm^{-1}, with a resolution of 2 cm^{-1}.

3.3.4 Scanning Electron Microscopy (SEM)

Scanning electron microscopy (SEM) is a widely utilized analytical technique that is typically employed to analyze the surface structure and characteristics of solid-state

samples. This method allows for detailed observation and study of the surface morphology of specimens at a high resolution. SEM enables researchers to examine the fine details and topographical features of materials with great precision, providing valuable insights into their composition and properties. By using SEM, scientists can gain a deeper understanding of the surface topography and structure of various materials, helping them make informed decisions about their properties and potential applications. This technique is especially useful in the fields of materials science, nanotechnology, and biological research, where the surface characteristics of specimens play a crucial role in determining their behavior and performance.

The scanning electron microscope (SEM) is a powerful tool used to produce three main types of signals: secondary electrons, backscattered electrons, and characteristic X-rays. Each of these signals provides valuable information about the sample being analyzed. Secondary electrons are low-energy electrons emitted from the surface of the sample in response to the electron beam. Backscattered electrons, on the other hand, are high-energy electrons that are reflected back from the sample. The characteristic X-rays, produced when the sample is bombarded with electrons, result from the inner shell electrons being displaced within the atoms. These signals work together to create a detailed image of the sample's surface, providing information about its composition and structure (Ul-Hamid, 2018). In this study, The investigation of powder and coating morphology was conducted utilising the Zeiss Gemini 560 instrument.

3.3.5 Differential Thermal Analysis - Thermogravimetric Analysis (DTA-TGA)

Differential thermal analysis (DTA) is a scientific method utilized to analyze the energy differences between a sample material and a reference material, typically over a period of time or as temperature changes. This technique allows researchers to observe and compare how the thermal characteristics of the sample material deviate from the standard reference material as the conditions are altered. By quantifying these energy differentials, scientists can gain valuable insights into the physical and chemical properties of the materials being studied. Differential thermal analysis is

commonly used in various fields, such as materials science, geology, and chemistry, to investigate phase transitions, thermal stability, and reaction kinetics. It is a versatile and powerful analytical tool that provides detailed information about the behavior of materials under different temperatures or time conditions. By plotting the energy differences against time or temperature, scientists can create a thermogram that visually represents the thermal behavior of the sample material. This allows for identifying key thermal events such as melting points, crystallization, or chemical reactions occurring within the material.

Thermogravimetry analysis (TGA) is a method used to analyze samples by monitoring the mass of the sample over time or temperature as the sample is subjected to a controlled temperature program. By plotting the data of mass loss or percent loss against either temperature or time, valuable insights into the chemical reactions taking place within the sample can be obtained. These reactions are typically depicted as one or more distinct steps, each indicating a change in mass (Brown, 2001).

A Shimadzu 60H model DTA-TG instrument was used for the DTA-TGA analysis of barley straw, SS solution, and dried composite mixture. The analysis was performed in the 25-700 ℃ range with a heating rate of 10℃/min under air atmosphere.

3.3.6 Surface Profilometry

In surface profilometry, an instrument is employed to amplify and record the vertical motions of a displacement stylus, which is displaced at a constant speed in order to measure the surface roughness. The stylus arm is positioned against the surface of the specimen, and the stylus is then moved across the surface using a scanning traverse unit at a constant speed. As the sample is moved, the stationary stylus passes over the surface of the specimen, detecting any surface irregularities by means of the transducer. The Ambios Technology XP-2 surface profilometer was used to measure the thickness of the coating.

3.3.7 Electrical properties

A current-voltage characteristic of a system is a fundamental concept in electronics, illustrating the relationship between electric current and voltage through a chart or graph. This relationship between the DC current passing through a device and the DC voltage across its terminals is crucial for understanding the behavior of electronic components. Engineers rely on these charts to analyze and determine key parameters of a device or material, as well as to predict how it will perform within an electrical circuit. These characteristics are commonly referred to as I-V curves, denoting the standard symbols for current and voltage.

In order to ascertain the current-voltage characteristic of the composite and to identify the insulation-conduction transition (percolation threshold) of the composite coatings, a Hall Effect device (Ecopia-HMS3000) was employed. The samples were prepared with graphite ratios of 1, 2, 3, 4, 5, 6, 7, 8, 9, 10, 12, 15, 20, 25, and 30 wt%. Furthermore, for the biochars, ratios of 5, 10, 15, 16, 17, 18, 19, 20, 25, and 30 wt% were employed to ascertain the percolation threshold of the composites. Additionally, the percolation threshold of a combination of two materials was investigated to ascertain the synergistic effect of the mixture.

3.3.8 Sensor properties

The performance of the sensors was investigated between 25 and 100°C. The samples were heated using a heating device, and the resistance and temperature changes were recorded using digital multimeters with data logging options. One of the multimeters (UNI-T, UT71D) was equipped with a thermocouple to record the temperature change, while the other was used to record the resistance change under heating (Mastech Ms8250d Digital Rms Multimeter) (Figure 3.2). The performance of the sensors was evaluated in terms of linearity, long-term stability, sensitivity, and response/recovery time.

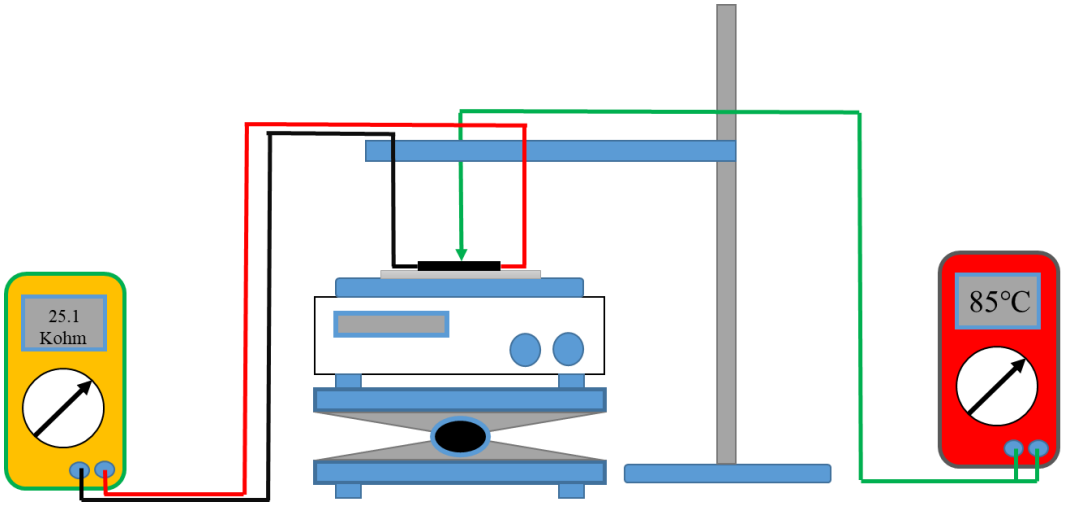

Figure 3.2 Test setup for measurement of resistivity change under heating and cooling conditions

CHAPTER FOUR
RESULTS AND DISCUSSIONS

4.1 Phase Analysis

Figure 4.1 presents the XRD patterns of graphite powder, dried SS solution powder, biochar, and composite (30Gr). It is evident that SS powders have an amorphous structure, whereas graphite powder exhibits a more crystalline structure. The sharp peak observed at 2θ = 26.5° and a small peak at 2θ = 54.5° represents (002) and (004) planes of graphite and indicate the typical crystal structure of graphite (JCPDS, 26-1079) (Ain et al., 2019; Siburian et al., 2018; Tarani et al., 2023). In the composite (30Gr), some amorphousness is observed due to the nature of the SS matrix. In the case of biochar, the broad band observed between 2θ = 20° and 30° indicates an amorphous carbon structure comprising randomly oriented graphitic layers. The sharp peak at 2θ = 26.6° can be attributed to the (002) plane of graphite-like structures (Dehkhoda et al., 2014; Yan et al., 2021).

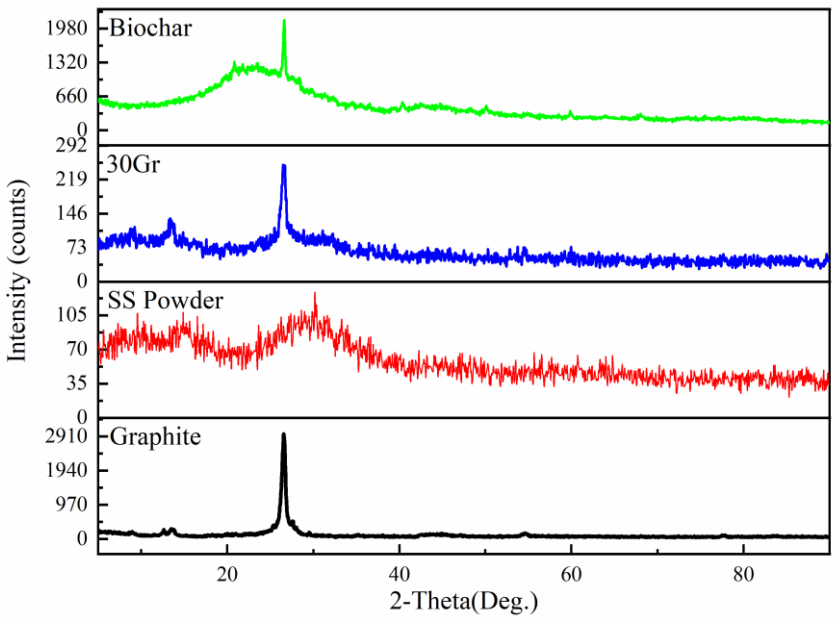

Figure 4.1 XRD patterns of biochar, graphite, composite and dried SS solution powder

4.2 Spectroscopic Analysis

Figure 4.2 illustrates the Raman spectra of the biochar, SS solution, graphite, and composite. The graphite and biochar exhibited the characteristic peaks associated with graphitic materials. The 1340 cm^{-1}, 1577 cm^{-1}, and 2673 cm^{-1} represent the characteristic D, G, and 2D peaks of graphitic materials, respectively. The D band is associated with defects in the carbon lattice and edge defects, while the G band is related to the vibration of in-plane carbon atoms. Additionally, the 2D peak located at 2673 cm^{-1} is significantly influenced by crystallinity and the number of graphene layers (Ferrari & Robertson, 2000; Yu et al., 2022). Regarding the SS solution, the region at 400-700 cm^{-1} indicates the bending vibrations of the Si-O bonds. The peak at 800-950 cm^{-1} associated with symmetric stretching vibrations of the Si-O bonds in the silicate tetrahedral. The main peak at 950-1100 cm^{-1} corresponds to symmetrical and asymmetric stretching of the Si-O-Si bridges in a silicate network, varying in oxygen content (Halasz et al., 2010; Ozgur Yasin Keskin & Erol, 2023b). Concerning composite (30Gr), it is clear that there are no more peaks than the main peaks of SS solution and graphite.

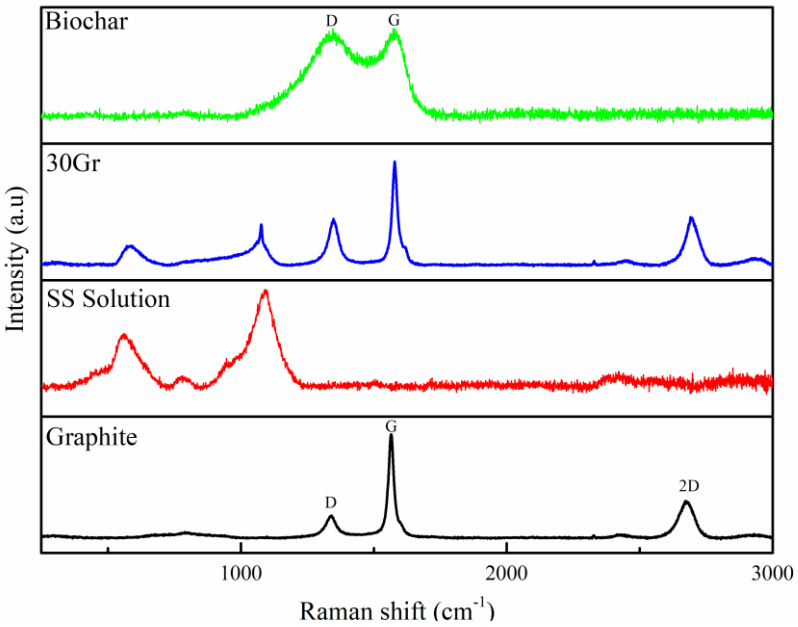

Figure 4.2 Raman spectra of biochar, SS solution, graphite, and their composite (30Gr)

4.3 FT-IR Results

The FT-IR spectra of barley straw and SS solution are shown in Figure 4.3. Firstly, in the spectrum of barley straw, the broad peak in the range of 3000-3700 cm^{-1} can be attributed to the O-H stretching vibrations in cellulose (Oh et al., 2005). The signals at 2919 cm^{-1} and 2850 cm^{-1} represent the C-H stretching vibrations of CH_2 and CH groups in cellulose and hemicellulose (Ozgur Yasin Keskin et al., 2024). The peak at 1730 cm^{-1} is associated with the C=O stretching vibrations of ester groups in hemicellulose and other carbonyl-containing groups (Uma Maheswari et al., 2012). O-H bending vibrations of water molecules are reflected in the peak at 1630 cm^{-1} (De Rosa et al., 2010). The peak at 1420 cm^{-1} can be related to the shearing or bending vibrations of CH_2 in cellulose and hemicellulose (O. Yasin Keskin et al., 2020). The small shoulders at 1316 cm^{-1} and 1371 cm^{-1} correspond to the C-H bending vibrations in cellulose and hemicellulose (Uma Maheswari et al., 2012). The C-O stretching vibrations of lignin are represented in the peak at 1250 cm^{-1} (Obi Reddy et al., 2009). The small shoulder at 1150 cm^{-1} is related to the C-O-C asymmetric stretching vibrations in cellulose and hemicellulose (Uma Maheswari et al., 2012). The strong peak at 1030 cm^{-1} is associated with the C-O stretching vibrations in cellulose and hemicellulose (Dalmis et al., 2020). As for the SS solution, the broad peak between 3700-2400 cm^{-1} is related to O-H stretching vibrations in silanol groups (Si-OH) and water molecules present in the solution (Morterra & Low, 1973). A small peak around 1650 cm^{-1} corresponds to the bending vibrations of water molecules . The intense peak between 900-1200 cm^{-1} is associated with the stretching vibrations of Si-O-Si bonds in silicate anions. The peak at 860 cm^{-1} can be related to the symmetric stretching vibrations of Si-O bonds (Chukanov & Chervonnyi, 2016).

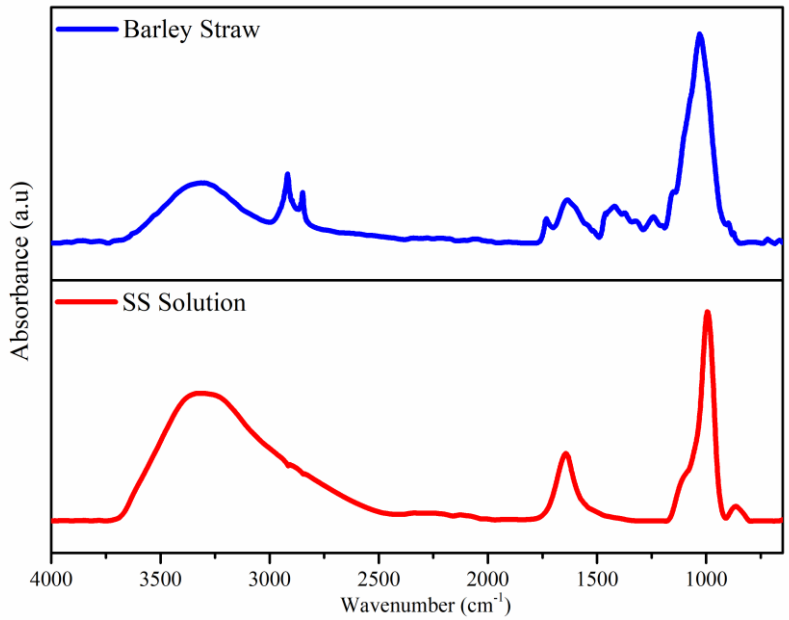

Figure 4.3 FT-IR spectrum of barley straw and SS solution

4.4 Morphology Analysis

Figure 4.4 shows the surface and cross-section morphology of barley straw, graphite, biochar, and coatings. Figures 4.4a and b show the surface and cross-section of raw barley straw. As shown in Figure 4.4a, barley straw has some protrusions on the surface, which can be related to the silica bodies on the outer shell. On the other hand, barley straw showed the typical structure with vascular bundles (Fig.4.4b) (Agbagla-Dohnani et al., 2003). Graphite particles are demonstrated in Figure 4.4c. The shape and size of graphite particles are highly variable. While flake graphite particles have a plate-like configuration, microcrystalline particles display an extensive range of morphologies. (Rew et al., 2017). On the other hand, Figure 4.4d presents the morphology of biochar particles. The image shows that biochar particles generally have plate-like structures with irregular shapes and smaller particle sizes than graphite (Dong et al., 2024; K. Su et al., 2023). Figures 4.4e and 4.4f illustrate the graphite-based and biochar-based coatings, respectively. In contrast to the variable morphology of the biochar and graphite particles, the coatings displayed a smooth and homogeneous surface morphology, indicative of the effective adhesion of the SS

matrix to the particles. In addition, the surface morphology of sample 5G-1B is given in Figure 4.4g. Clearly, coatings with a combination of graphite and biochar particles also have a smooth surface (Verma et al., 2023).

Table 4.1 Elemental composition of samples.

	Elemental Composition (wt. %)						
Sample	**Na**	**Si**	**C**	**O**	**K**	**Ca**	**Cl**
Barley Straw	-	1.1	51.3	44.8	2.5	0.4	-
30Gr	23.2	18.5	13.3	42.1	-	-	-
25Bc	12.6	20.4	20.8	41.2	1.5	0.6	0.3
5G-1B	22.9	14.2	11.3	49.0	0.1	-	-

The elemental compositions of barley straw and the coatings are listed in Table 3.2. Barley straw mainly consists of C, O, and a minor amount of Si. On the other hand, graphite-based samples included three major elements (Na, Si, C, and O), while biochar-based samples contained four major elements (Na, Si, C, and O) with three minor elements (K, Ca, and Cl).

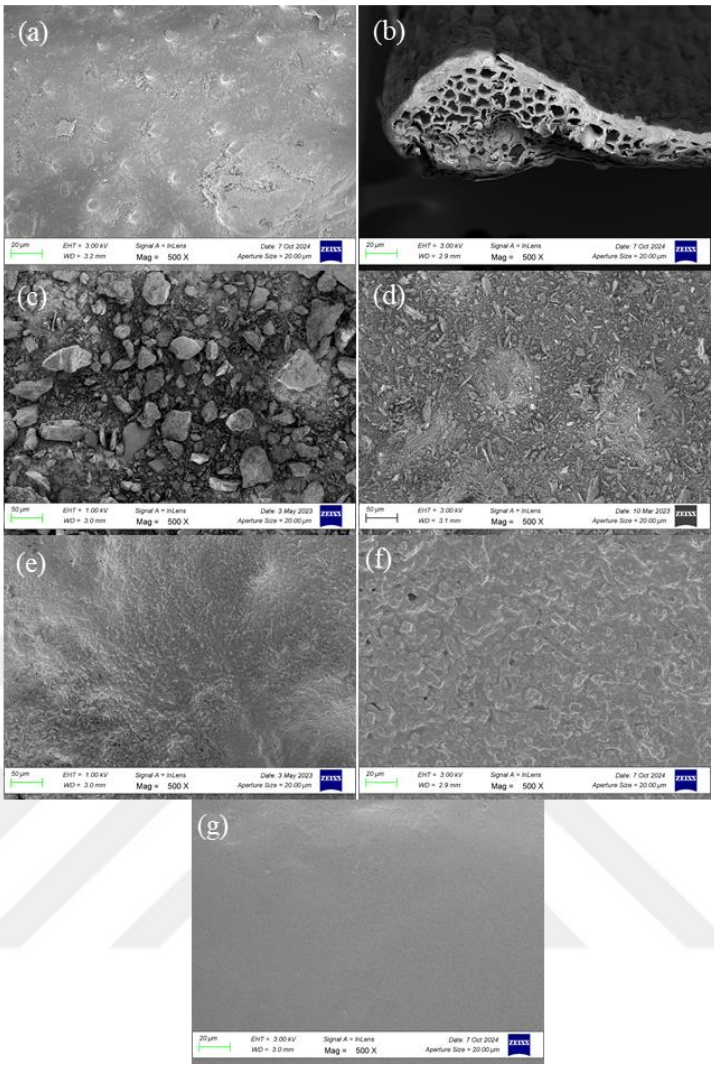

Figure 4.4 SEM images of (a) Barley straw, (b) Cross-section of barley straw, (c) graphite, (d) biochar, (e) Sample 30Gr, (f) Sample 25Bc, (g) Sample 5G-1B

Elemental mapping of samples were given in Figure 4.5. Figure 4.5a and b represents the elemental distribution of composite coating of 20Gr and 30Bc. As seen in image Carbon (C), Sodium (Na), and Silicon (Si) distributed homogeneously.

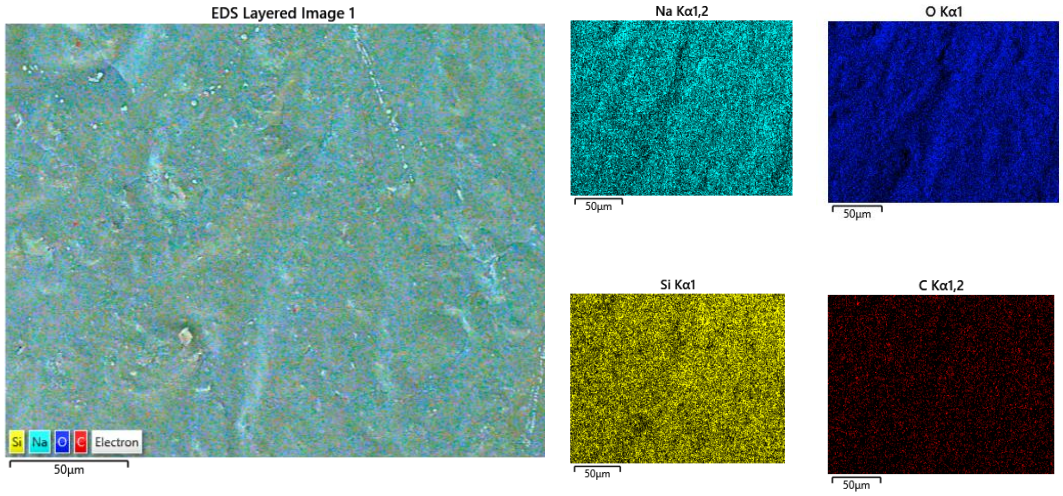

(a)

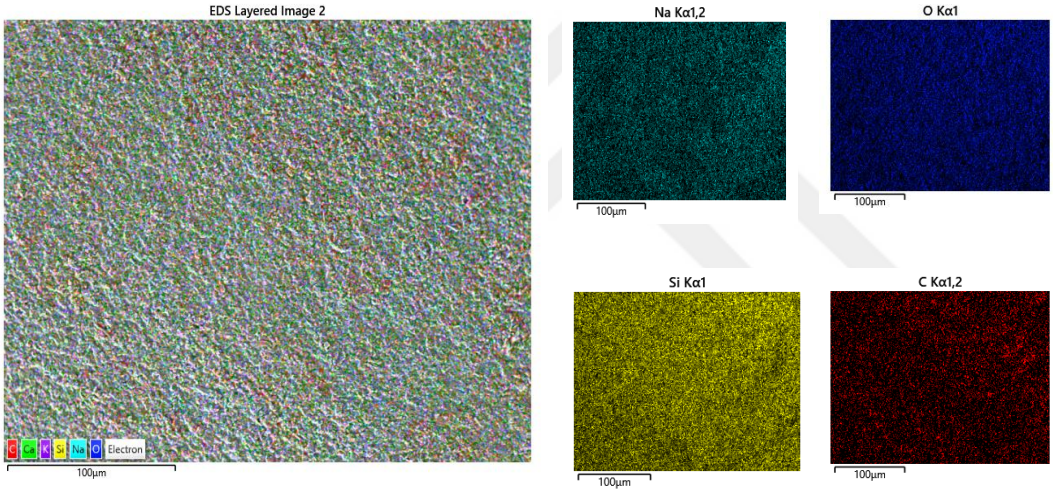

(b)

Figure 4.5 Elemental mapping of (a) 20Gr and (b) 30Bc

4.5 Thermal Analysis

Figure 4.6 presents the thermal analysis of the dried composite, and barley straw. Figure 4.6a presents the thermal analysis of the dried composite (30Gr). To ascertain the suitability of composite as temperature sensors, it is important to understand their thermal behavior in the composite. In particular, for the working range of the sensors (25-100 °C), it is of the utmost importance that the sensor materials do not exhibit any weight loss or degradation in terms of stability and repeatability following the drying

process. As illustrated in Figure 4.6a, no significant weight loss was observed until approximately 180 ℃. In particular, within the 25-100 ℃ range, the composite mixture did not exhibit any weight change. The first peak at nearly 185 ℃ can be related to the evaporation of absorbed water by graphite and chemically bonded water in SS. The second peak at almost 680 ℃ can be associated with the melting of silica catalyzed by Sodium and the formation of bulk silica (Le & Le, 2021).

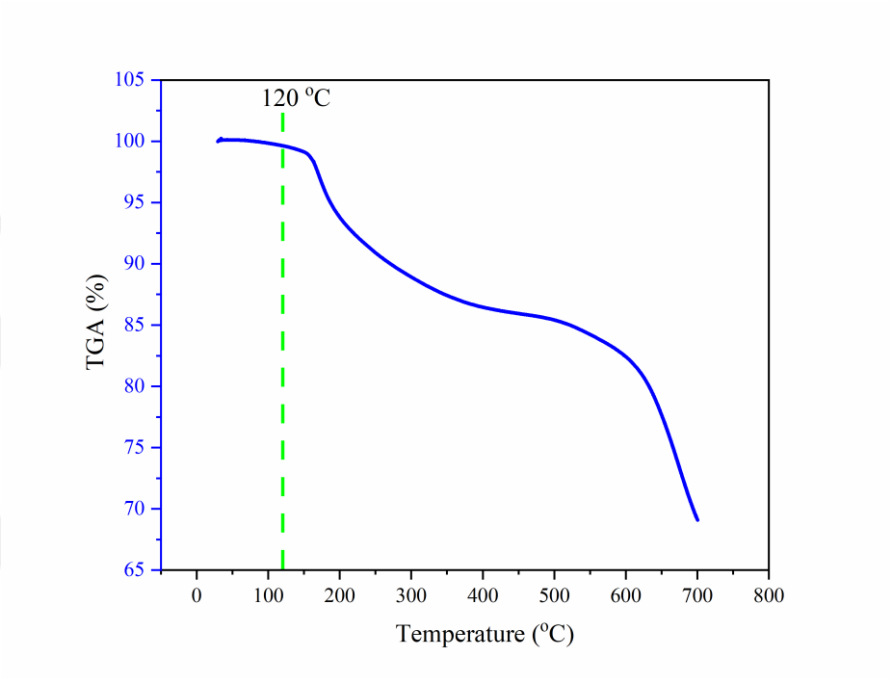

(a)

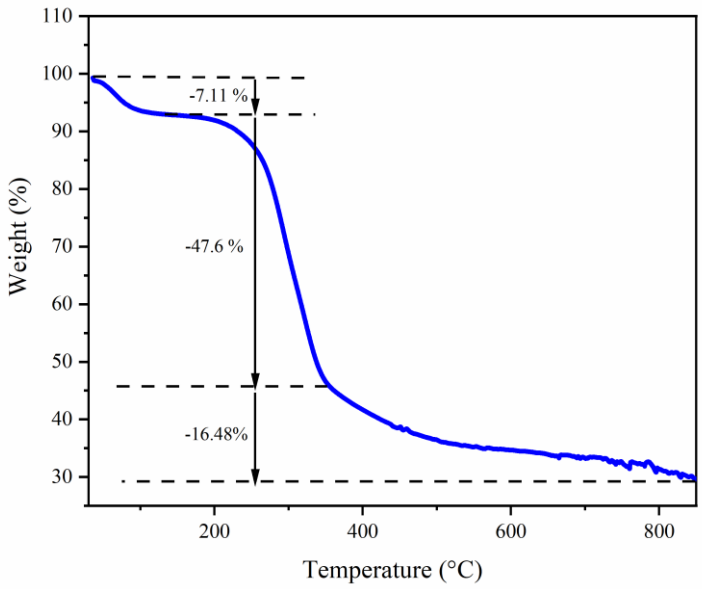

(b)

Figure 4.6 TG curves of (a) Dried composite, (b) barley straw

Figure 4.6b shows the thermal analysis of barley straw in the range of 25-850 ℃. The first mass loss is due to water evaporation, with a weight loss of 7.11% (Ridzuan et al., 2016). The largest weight loss of 47.6% is related to the decomposition of cellulose, and the rest of the weight loss (16.48%) is associated with the residual fiber content (Saravanakumar et al., 2013). After 800℃, no more weight loss was observed, and 800℃ was determined as pyrolyzing temperature in terms of crystallinity and conductivity.

4.6 Surface Profile

The surface profile of sample 30Gr composite coating is illustrated in Figure 4.7. It is evident that the coating does not have a smooth surface. On the contrary, coatings displayed irregularities on the surface, and the thickness of coatings was in the range of 50-100μm. Additionally, an accumulation was observed at the edge of the coatings

due to the edge effect. However, beyond the edges, the surface profile remained until the end of the coating.

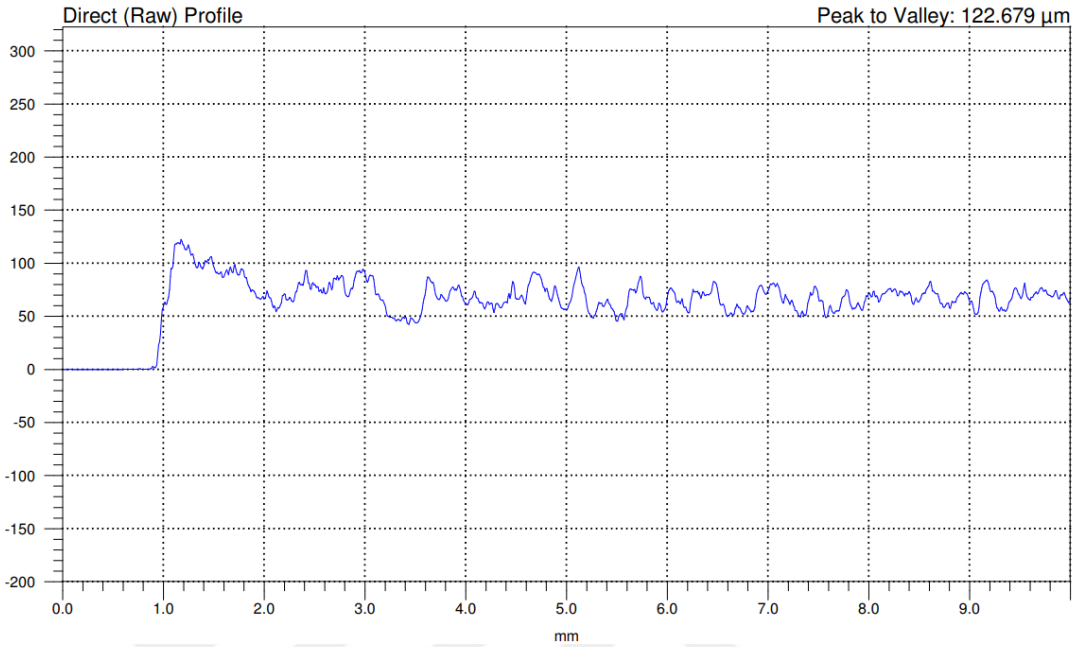

Figure 4.7 Surface profile of 30Gr

4.7 Electrical Properties

The percolation threshold in conductive composites denotes the critical concentration of conductive filler particles where the composite undergoes a transition from insulating to conductive behavior. This phenomenon holds significant importance in the optimization and comprehension of electrical conductivity within composite materials, particularly in fields such as electronics, sensor technologies, and electromagnetic shielding. Achieving a precisely controlled percolation threshold is paramount for the development of sensors capable of ensuring sensitivity and stability in diverse applications, including environmental monitoring and biomedical sensing (Vieira et al., 2022).

Figure 4.8 illustrates the electrical conductivity of graphite-based composites, biochar-based composites, and their combination. Figure 4.8a depicts the electrical conductivity of graphite-based composites. As observed in Figure 4.8a, the samples

exhibited high resistivity, or insulating behavior, until 7 wt. %. Following this, a notable increase in conductivity was observed in the mixture. As previously stated, the instantaneous rise in conductivity signifies the percolation threshold of the mixtures. The percolation threshold of the graphite-based samples was determined to be nearly 7.5 (wt. %). Compared to the literature, lower percolation threshold values were obtained with graphite-based samples (Arman Kuzubasoglu & Kursun Bahadir, 2020b; Phadkule & Sarma, 2023b). This decrease in percolation threshold can be explained by the addition of SS solution. When used as a component of the composite matrix, sodium silicate can alter the structure and interface between conductive fillers, potentially enhancing the formation of conductive pathways. Sodium silicate, when used in appropriate concentrations and formulations, can improve the dispersion and alignment of conductive fillers within the composite. By facilitating better contact between fillers, sodium silicate can reduce contact resistance and promote the formation of a percolative network at lower filler concentrations (Chiao et al., 2021; Shen et al., 2006). Similar experiments were performed for biochar-based composites (Figure 4.7b). For biochar-based samples, the percolation threshold of samples was determined to be nearly 16.5 (wt. %). The conductivity and percolation threshold differences between graphite and biochar-based composites can be associated with the crystallinity of powders (Bartoli et al., 2022; Kane et al., 2021).

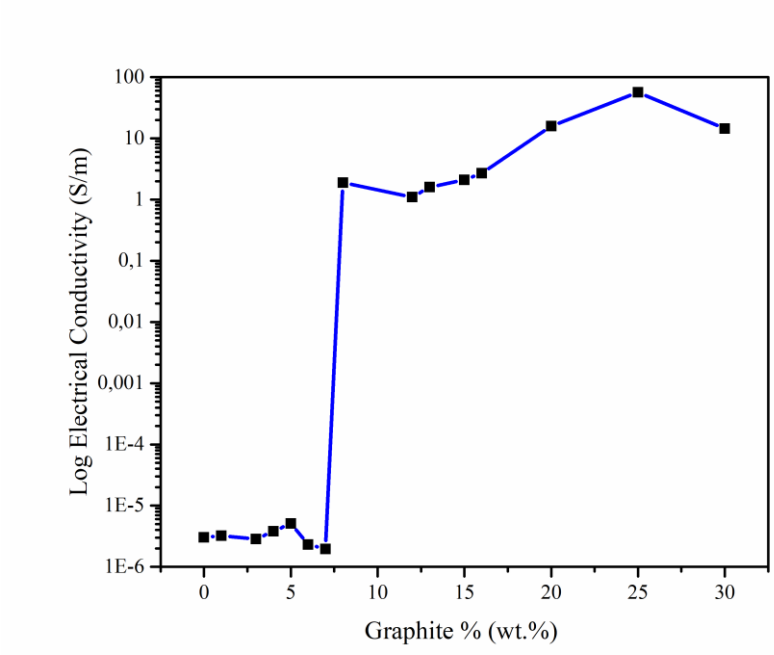

(a)

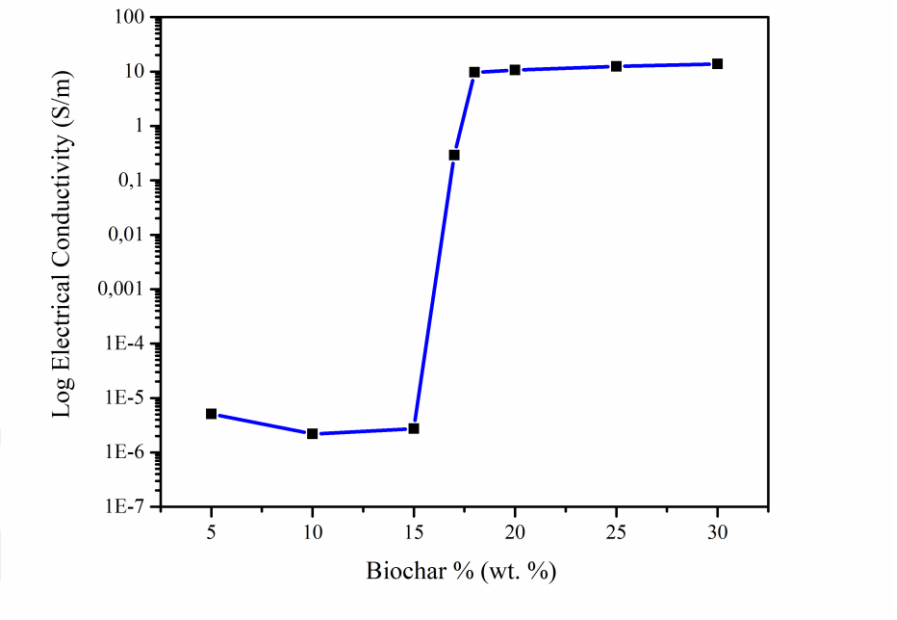
Log Electrical Conductivity (S/m)
100
10
1
0,1
0,01
0,001
1E-4
1E-5
1E-6
1E-7
5
10
15
20
25
30
Biochar % (wt. %)

(b)

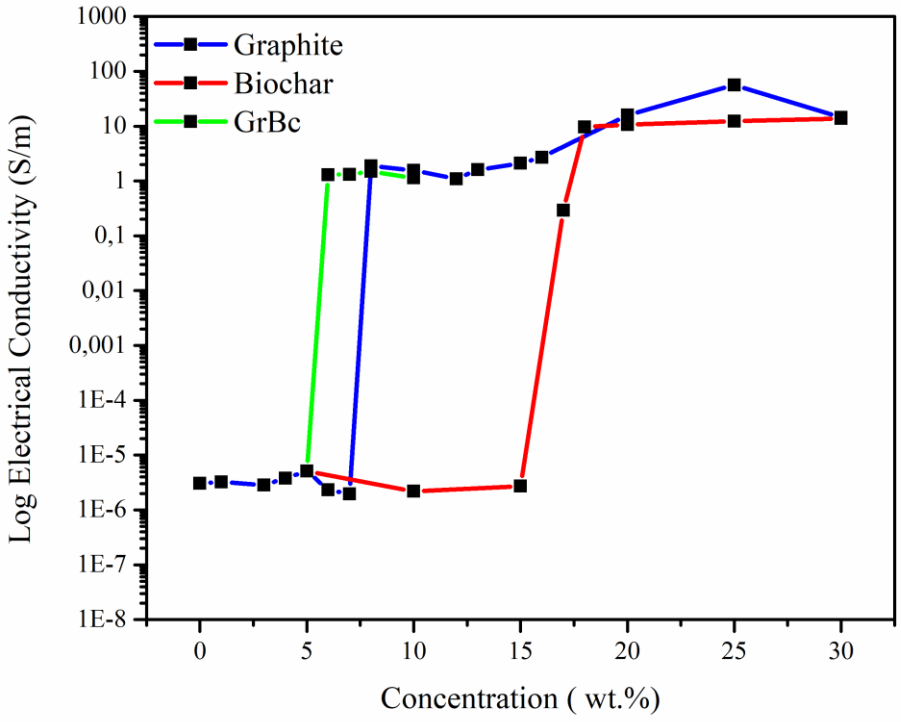

(c)

Figure 4.8 Electrical conductivities of (a) Graphite, (b) Biochar, and (c) Graphite/biochar-based composites

On the other hand, the synergetic effect of biochar and graphite was investigated and compared with bare graphite and biochar-based composites (Figure 4.8c). For investigation, graphite and biochar were mixed with different ratios and their conductivities were measured. As seen in the figure, while sample 5G-OB behaves like insulating material, an instantaneous increase was observed in sample 5G-1B. After sample more biochar addition to composite, no more increase was observed in conductivity. Within this framework, the percolation threshold of graphite/biochar samples was determined as 5.5 (wt. %). It is clear that the synergetic effect positively affected the conductivity of samples. This phenomenon can be explained by the co-percolation. In contrast to the conventional percolation theory, which typically examines the connectivity of a single type of component, co-percolation extends this concept to encompass the interactions between multiple types of components or

systems (R. Chen et al., 2013). As previously stated, biochar powders exhibit a lower particle size than graphite powders. In this context, biochar particles can act as a bridge between graphite particles, filling the gaps between them. Consequently, this phenomenon can result in an increase in the total electrical conductivity of the system.

4.8 Sensor Performance

4.8.1 Graphite Based Samples

The sensor performance of the samples was investigated in terms of linearity, stability, and repeatability. Figure 4.9 shows the response of the sensor as a function of temperature. As can be seen, the samples exhibited a decrease in resistance with an increase in temperature, demonstrating negative temperature coefficient (NTC) behaviour. Furthermore, a linear behaviour was observed in samples under heating and cooling conditions. The increase in conductivity can be explained by an increase in the mobility of electrons or more electrons can be excited from the valance band to the conduction band (Phadkule & Sarma, 2023b). On the other hand, due to the very low thermal expansion coefficient of glass (Kompan et al., 2008), samples exhibit linear behavior. As previously stated, the sensitivity of the sensor is typically quantified by the temperature coefficient of resistance (TCR). The sensitivities of samples were calculated as −0,01/°C, − 0,0479/°C, and − 0,0432/°C for 10Gr, 15Gr, and 20Gr, respectively.

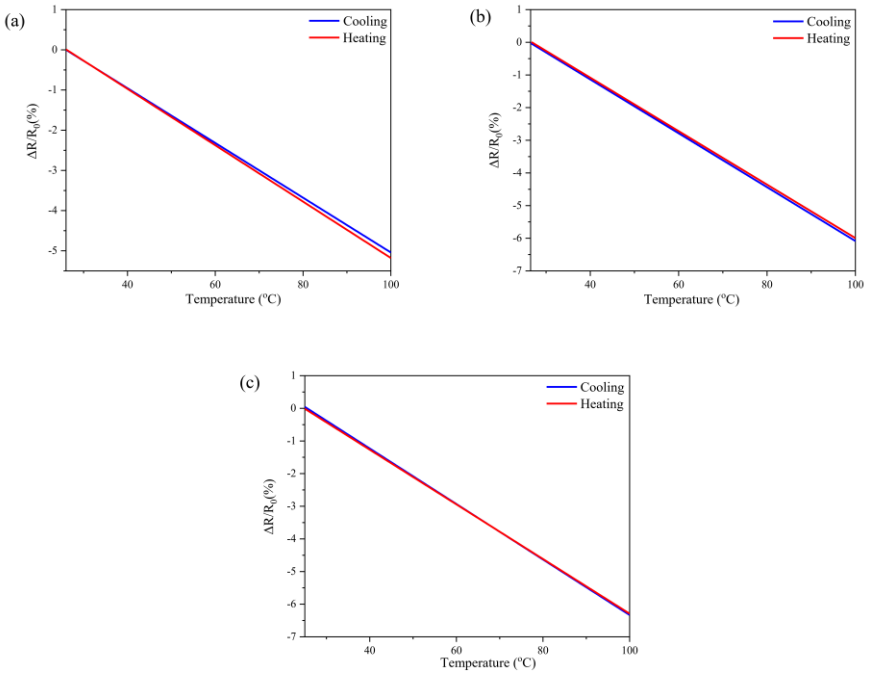

Figure 4.9 Normalized response of (a) 10Gr, (b) 15Gr, (c) 20Gr samples on glass substrate between 25–100 °C

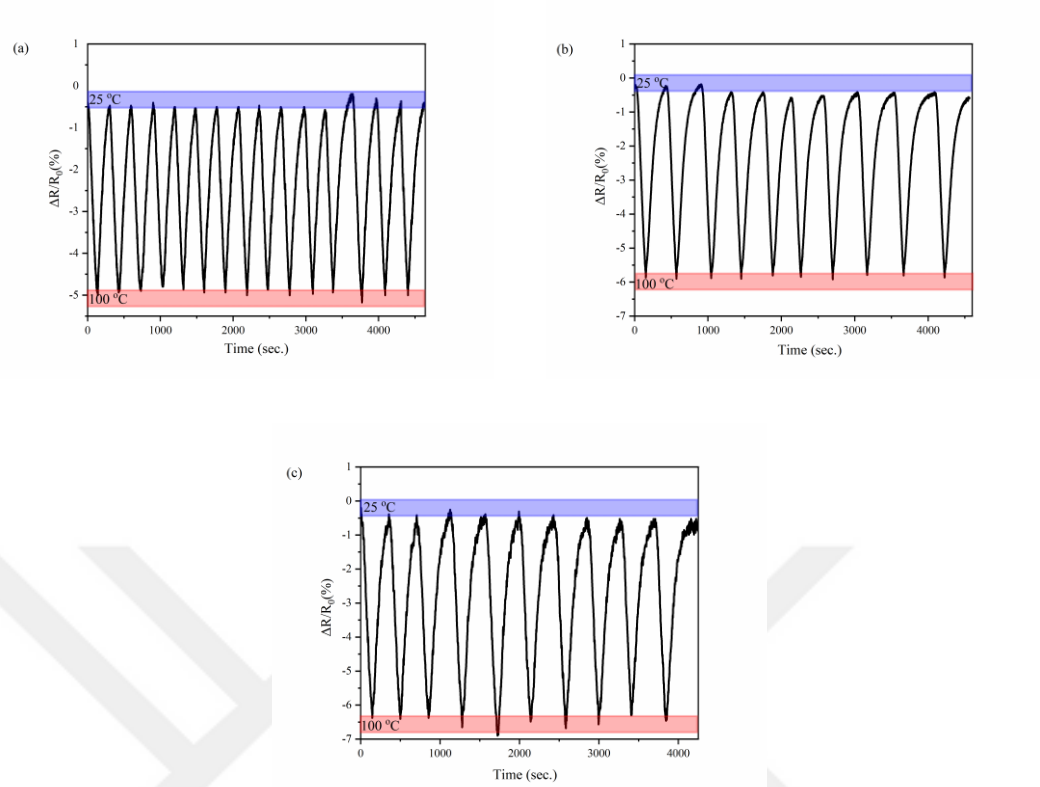

Figure 4.10 Repeatability of (a) 10Gr, (b) 15Gr, (c) 20Gr samples on glass substrate between 25–100 °C

Figure 4.10 presents the results of the repeatability tests conducted on graphite-based samples. Tests were conducted with multiple heating and cooling cycles, with the temperature increasing from room temperature to 100 °C. As shown in the figure, all samples demonstrated good repeatability between 25 and 100 °C. Upon comparison of the samples, evident from the number of cycles increased in direct proportion to the reduction in graphite ratio at a fixed time interval. Figure 4.11 presents the results of long-term stability tests on samples. The tests were conducted at constant temperatures (25-100 °C) for a fixed duration (180 sec.). As can be observed, the samples exhibited near-linear behavior at varying temperatures. Moreover, the response and recovery time of samples were measured. Figure 4.12 presents the response and recovery time of samples. It can be seen that the 10Gr sample shows the lowest response and recovery time (30/48 seconds, respectively). With the increasing filler concentration, the response and recovery time of samples increased (35/70 seconds for 15Gr and 48/70 seconds for 20Gr). An increase in response and recovery time can be related to thermal

diffusion. Graphite has high thermal and electrical conductivity, so increasing graphite concentration makes the composite more electrically and thermally conductive. While this might seem like it would reduce response and recovery time, the opposite occurs because thermal diffusion becomes slower in denser conductive particle networks. The composite may take longer to achieve uniform thermal distribution, causing a delay in the response of resistivity to temperature changes (Mohammad et al., 2022).

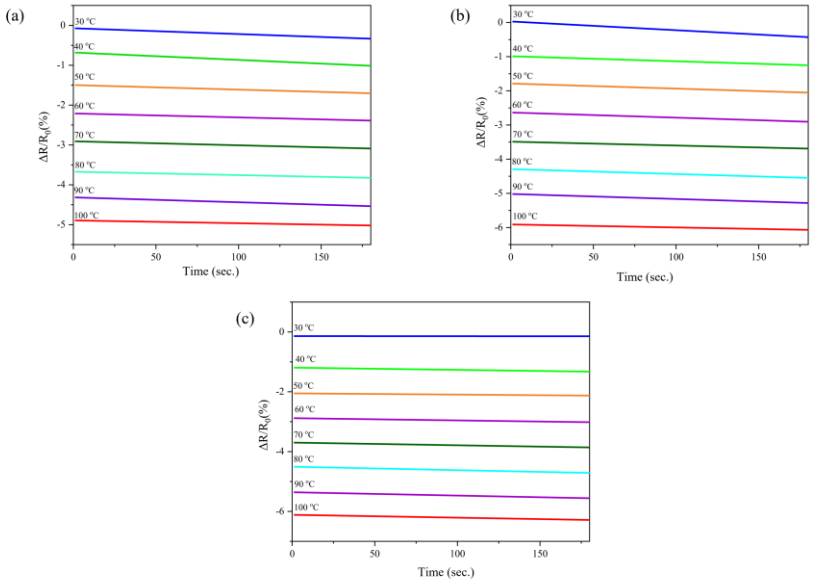

Figure 4.11 Long-term stability of (a) 10Gr, (b) 15Gr, (c) 20Gr samples on glass substrate

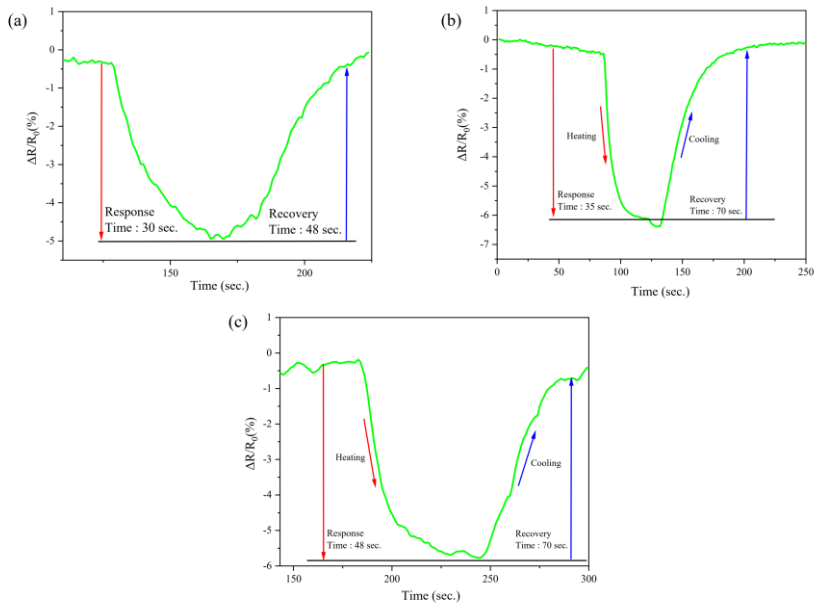

Figure 4.12 Response and recovery time of (a) 10Gr, (b) 15Gr, (c) 20Gr samples on glass substrate

On the other hand, similar experiments were performed on PVC flexible substrate to investigate the potential usage of composite in flexible applications. Figure 4.13 illustrates the temperature-dependent variation in normalized resistivity for the samples under consideration. The samples exhibited NTC behavior, indicating that the resistance of the samples decreased with increasing temperature. Furthermore, in comparison to the samples on the glass substrate, it is clear that the samples on a PVC substrate exhibited non-linear behavior. This phenomenon can be attributed to the expansion of the polymer substrate. It is well known that polymers expand with increasing temperature, and as they do so, adjacent particles in composite structures move away from each other, thereby increasing the resistivity of the composite structure (Geng et al., 2022; B. Wang et al., 1997). Conversely, an increase in temperature decreases the resistivity of composite material due to an increase in the mobility of electrons or a higher number of electrons at the conduction band (Phadkule & Sarma, 2023b). This opposition between the substrate and the composite material can cause non-linear behavior under heating conditions. Furthermore, in comparison to the concentration of graphite, it is evident that the sample with the highest amount of graphite exhibits a more linear behavior. This phenomenon can be attributed to an

increase in the contact point between adjacent graphite particles in the composite structure.

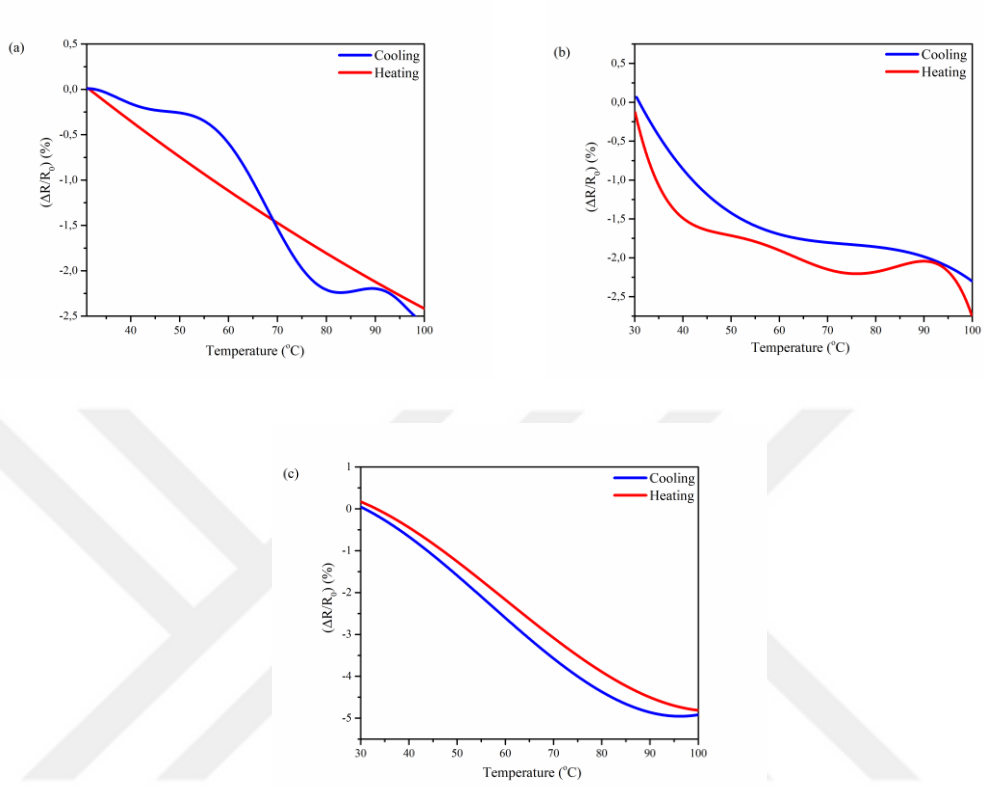

Figure 4.13 Normalized response of (a) 10Gr, (b) 15Gr, (c) 20Gr samples on PVC substrate between 25–100 °C

Figure 4.14 depicts the results of a repeatability test conducted on samples. As evidenced by the figure, all samples demonstrated repeatability within a temperature range of 25–100 °C. Upon comparative analysis, it became evident that as the concentration of graphite increased, the sensors exhibited enhanced repeatability. Additionally, some resistivity variations were observed in sample 10Gr, which can be attributed to low graphite concentration and deterioration of contact points at the composite material after multiple cycles. A comparison of samples on the glass and PVC substrates reveals that the samples on glass substrate exhibited superior repeatability due to the low thermal expansion properties of glass. Figure 4.15 illustrates the long-term stability of the samples. As can be observed in the figure, while the samples exhibited linear behavior at low temperatures, they did not exhibit linear behavior at higher temperatures. When samples are compared, the sample with

the highest amount of graphite exhibited the best long-term stability over the given time period.

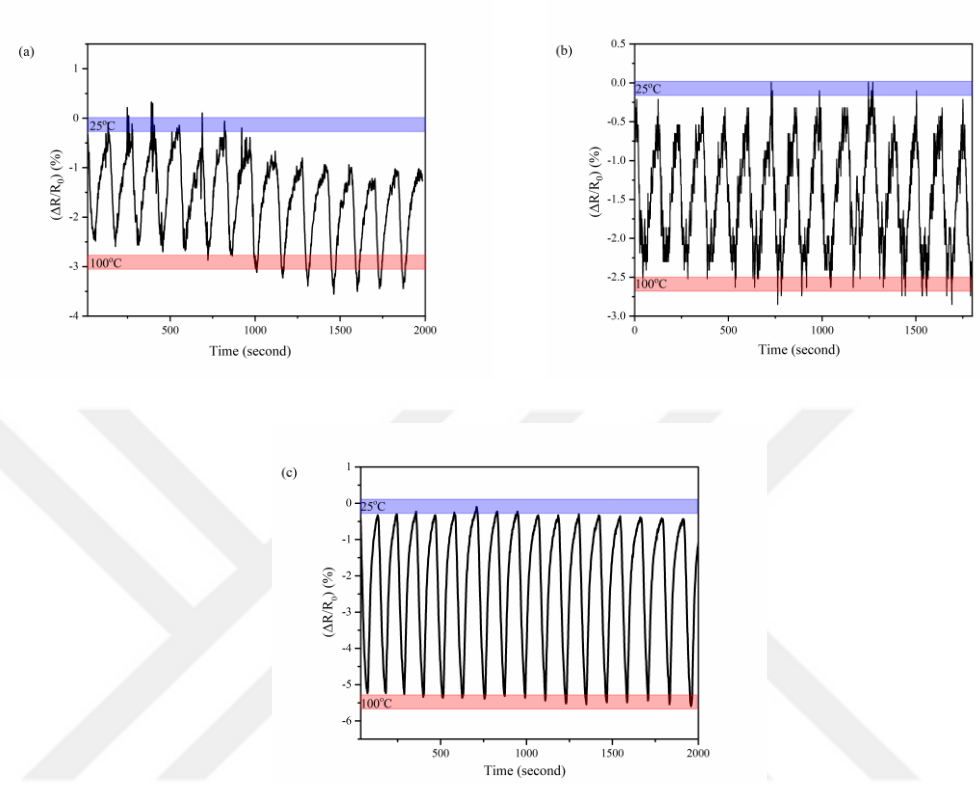

Figure 4.14 Repeatability of (a) 10Gr, (b) 15Gr, (c) 20Gr samples on PVC substrate between 25–100 °C

A comparative analysis of samples on glass and PVC substrates in terms of long-term stability indicates that samples on glass substrates demonstrate superior stability. This phenomenon in samples with PVC substrates can be attributed to the deterioration of the substrate over time, which also results in the degradation of the composite material. These deformations in the sensor material lead to a change in resistance within the structure, ultimately causing instability. Figure 4.16 illustrates the response and recovery time of the samples on the PVC substrate. As can be observed in the figure, the response time of the sensors increased and the recovery time decreased in general with increasing concentration. Increase in response time can be related to the decreasing thermal diffusion at denser carbon network (Mohammad et al., 2022). On

the other hand, decrease in recovery time can be associated with restriction of thermal expansion of PVC substrate by the high concentration of graphite.

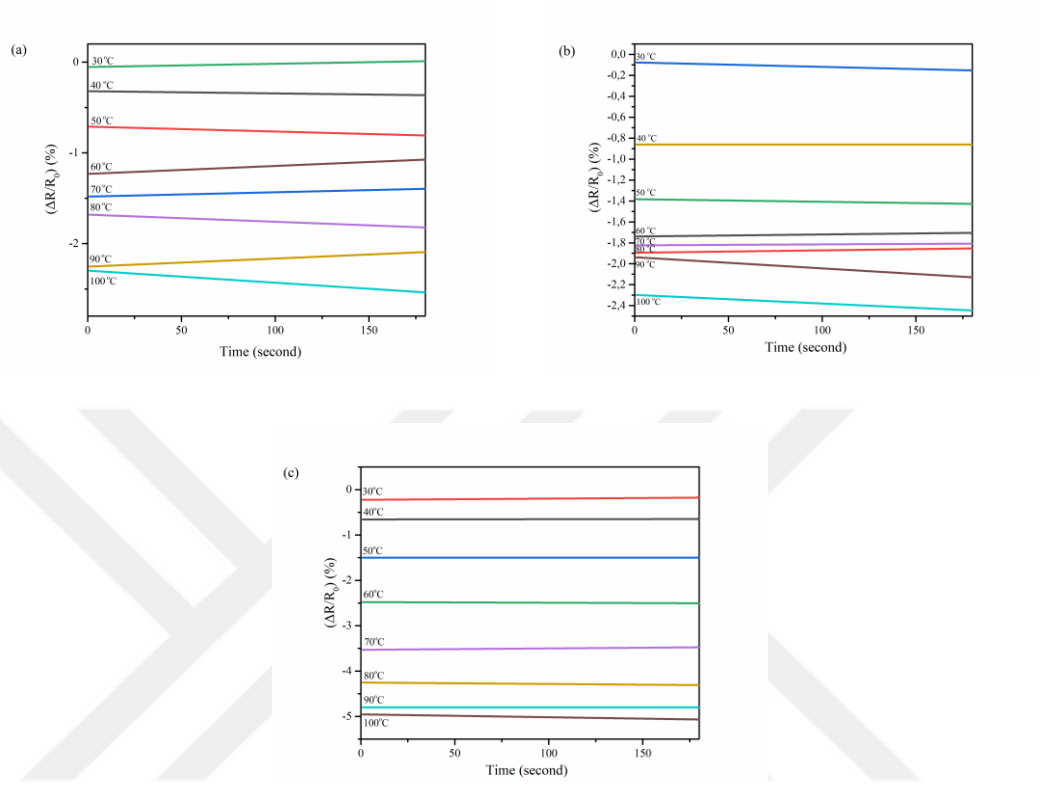

Figure 4.15 Long term stability of (a) 10Gr, (b) 15Gr, (c) 20Gr samples on PVC substrate

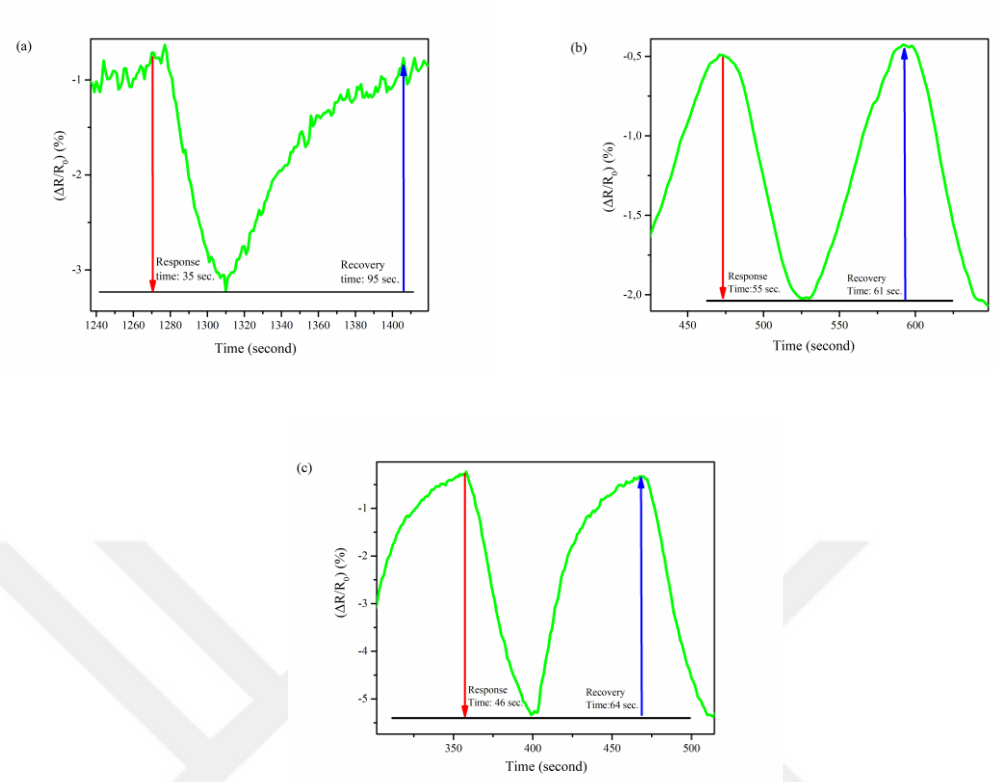

Figure 4.16 Response and recovery time of (a) 10Gr, (b) 15Gr, (c) 20Gr samples on PVC substrate

4.8.2 Biochar-Based Samples

Experiments on temperature-sensing properties were conducted for biochar-filled composites coated on glass substrates. 20Bc, 25Bc, and 30Bc samples were chosen due to the percolation threshold of biochar samples (nearly 16.5 wt. %). Figure 4.17 presents the heating and cooling response of biochar-based composite samples on the glass substrate as a function of temperature. As seen in the figure, samples exhibited linear or nearly linear behavior while heating and non-linear behavior while cooling. Also, some degree of deviation was observed for onset and final resistance.

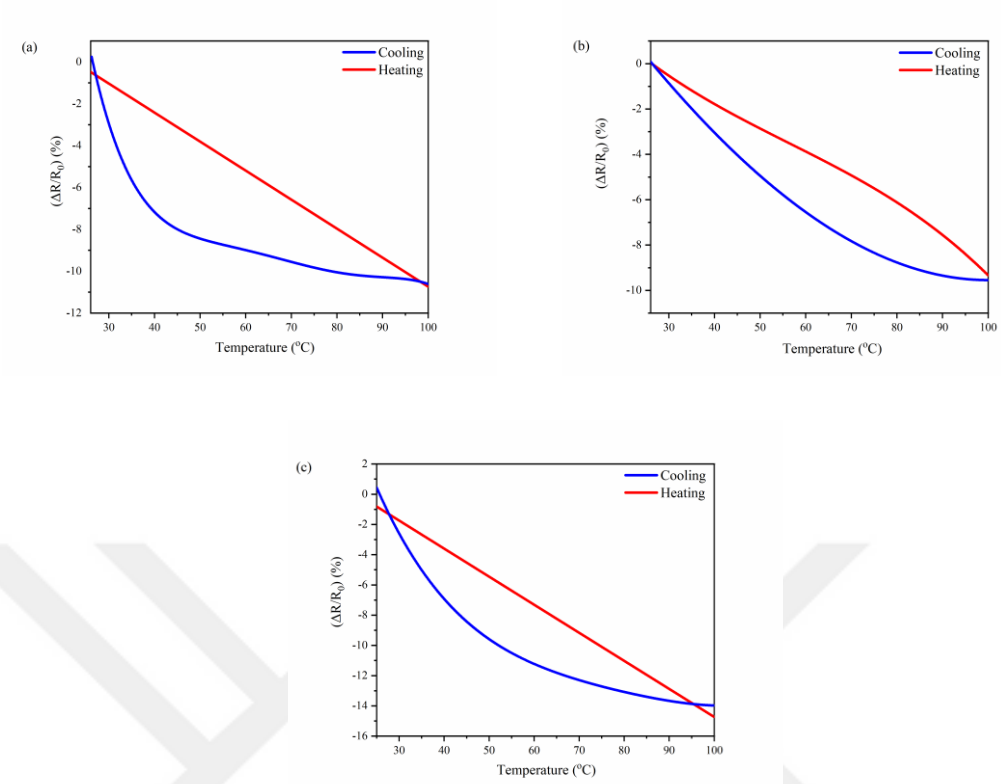

Figure 4.17 Normalized response of (a) 20Bc, (b) 25Bc, (c) 30Bc samples on glass substrate between 25–100 °C

It is evident that natural graphite and biochar exhibit distinct behavior in their heat-releasing properties, which can be attributed to their varying structures and crystallinity. This non-linear behavior can be associated with the crystallinity of biochar. The heating and heat-releasing properties of biochar are closely linked to its crystallinity. Higher crystallinity generally enhances thermal conductivity, thermal stability, and electrical conductivity, making biochar more effective in heat dissipation (S. Liu et al., 2022). In comparing graphite and biochar. Consequently, graphite-based samples demonstrate a more linear behavior than biochar-based samples on the glass substrate.

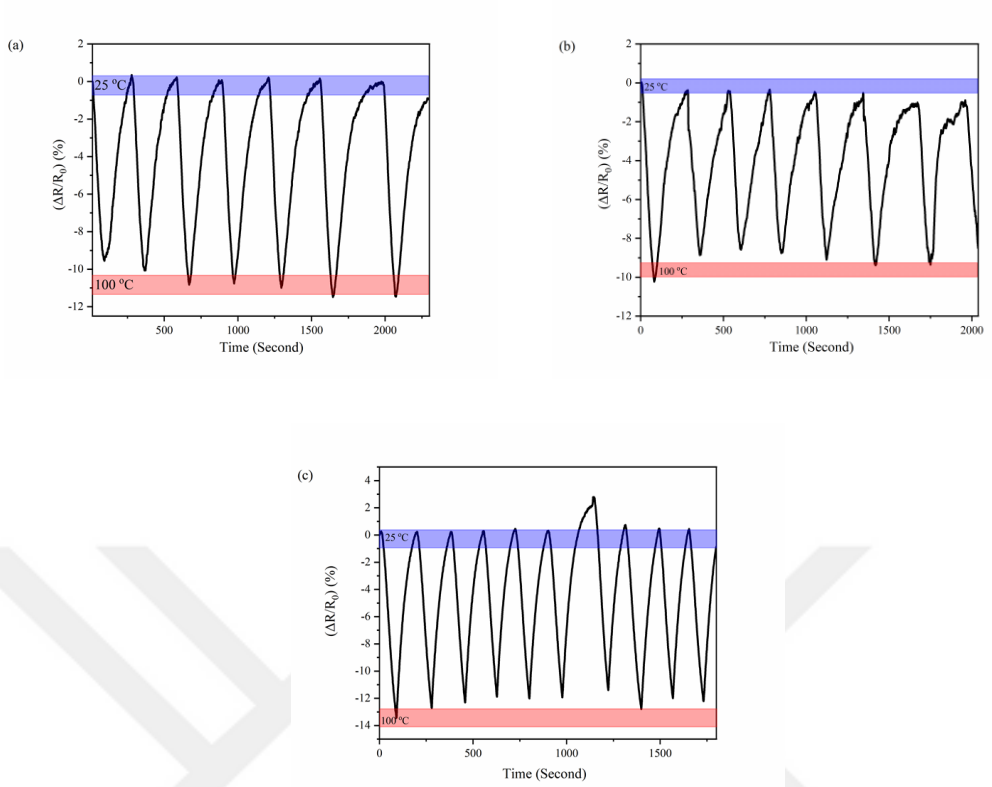

Figure 4.18 Repeatability of (a) 20Bc, (b) 25Bc, (c) 30Bc samples on glass substrate between 25–100 °C

Figure 4.18 presents the results of the repeatability tests conducted on biochar-based samples. As illustrated in the figure, the samples exhibited consistent performance across from room temperature to 100 °C. Upon comparing the samples, it became evident that the number of cycles increased with an increase in biochar concentration. This phenomenon can be attributed to the fact that a higher concentration of biochar particles results in a greater number of contact points within the composite structure, thereby enhancing the overall conductivity of the material (Mohd Radzuan et al., 2017). The long-term stability results of the samples are given in Figure 4.19. The stability of samples was conducted at a fixed temperature between room temperature to 100 °C for a fixed period of time (180 s.). All samples showed long-term stability at various temperatures.

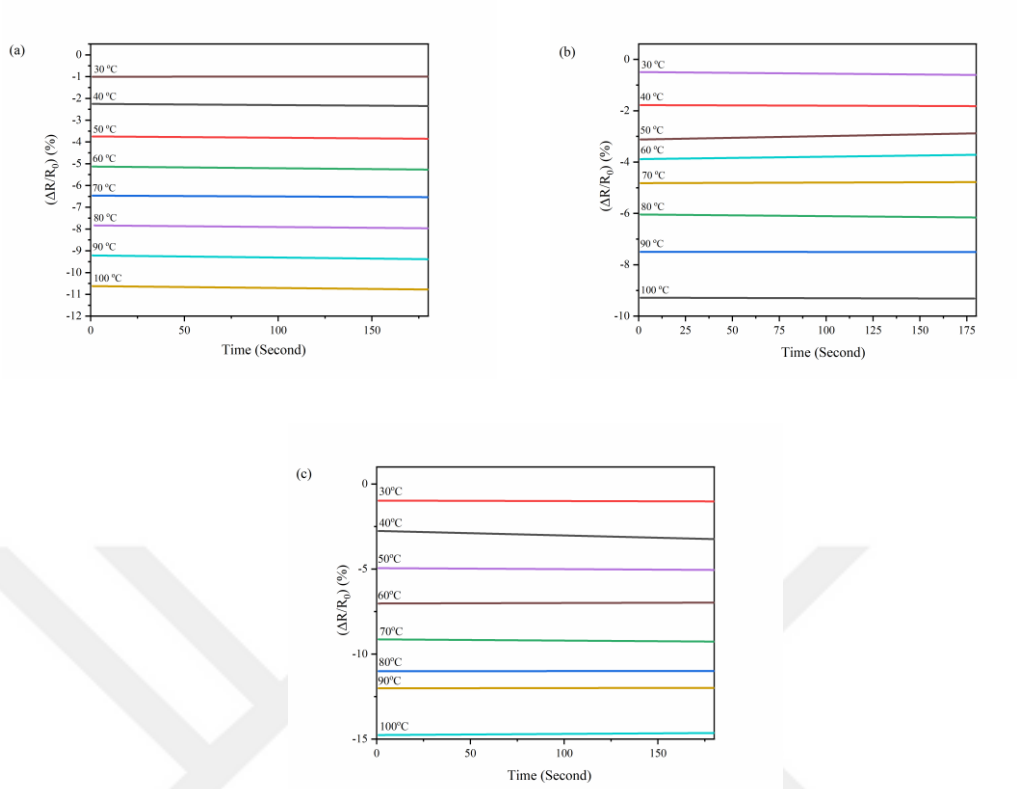

Figure 4.19 Long-term stability of (a) 20Bc, (b) 25Bc, and (c) 30Bc samples on glass substrate between 25–100 °C

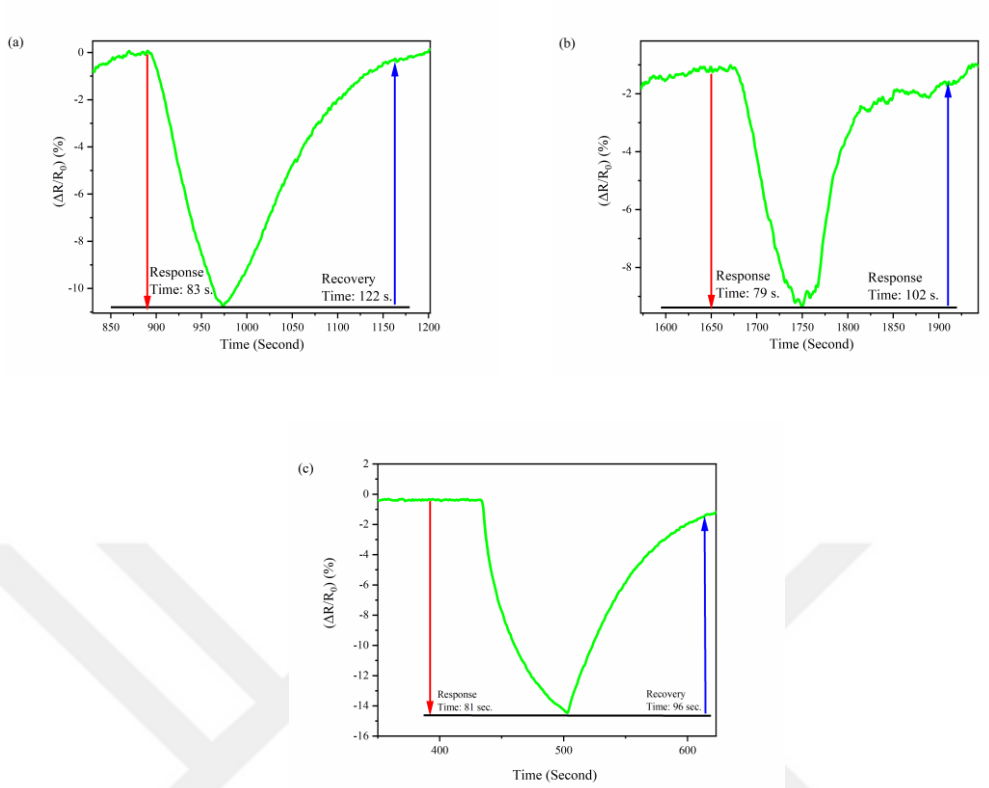

Figure 4.20 Response and recovery time of (a) 20Bc, (b) 25Bc, (c) 30Bc samples on glass substrate between 25–100 °C

Figure 4.20 shows the response and recovery times of biochar-based samples. While sample 25Bc exhibited similar response and recovery times, other samples showed differences between response and recovery time. On the other hand, some decrease was observed in response and recovery time at 25Bc but again increased at 30Bc. In comparing graphite and biochar-based samples on a glass substrate, it is clear that graphite-based samples exhibited lower response and recovery time. This difference can explained by the crystallinity differences between graphite and biochar. The thermal and electrical conductivity of carbon-based materials is strongly correlated with the crystallinity of carbon-based materials. Due to the high crystallinity of graphite, graphite-based samples exhibited better performance in terms of response and recovery time (S. Liu et al., 2022).

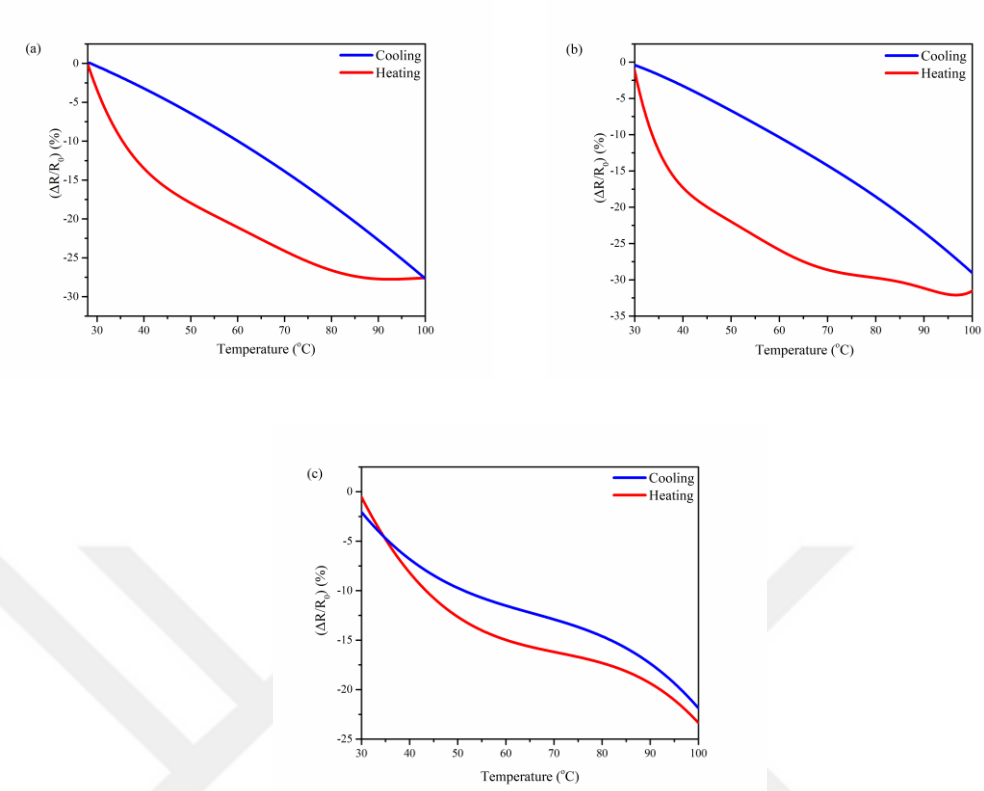

Figure 4.21 Normalized response of (a) 20Bc, (b) 25Bc, (c) 30Bc samples on PVC substrate between 25–100 °C

Figure 4.21 illustrates the heating and cooling response of the biochar-based composite as a function of temperature. As can be seen from the figure, the samples exhibited non-linear behavior in response to temperature. Regarding biochar concentration, 30Bc is the best sample due to the similar or nearly the same heating and cooling response. When biochar-based samples were compared in terms of substrate, almost similar behaviors were observed. Compared with graphite on PVC substrate, biochar-based samples exhibited better performance in terms of linearity. This phenomenon can be explained by the particle sizes of conductive filler. As mentioned before, graphite powders have larger particle sizes than biochars'. Under heating conditions, the polymer substrate expands, and conductive particles move away from each other. Due to the big particle sizes of graphite, the conductive pathway can be damaged easily. As for biochar-based samples on PVC substrate, due to small particle sizes, they can form more conductive pathway and they can fill the gaps between large particles and provide a better conductive pathway for composite.

Additionally, the distance between adjacent particles decreases with decreasing particle size (Jing et al., 2000; Özmihçi & Balköse, 2013; Xue, 2004). Figure 4.22 shows the repeatability test of biochar-based samples on PVC substrate. It is clear that all samples exhibited good repeatability, but some resistivity change was observed in sample 30Bc. In terms of biochar concentration, the number of cycles increased with increasing biochar concentrations at a given period of time. These results are also compatible with the response and recovery time results of samples. Compared to graphite-based samples on PVC substrate, biochar-based samples exhibit better cyclic performance.

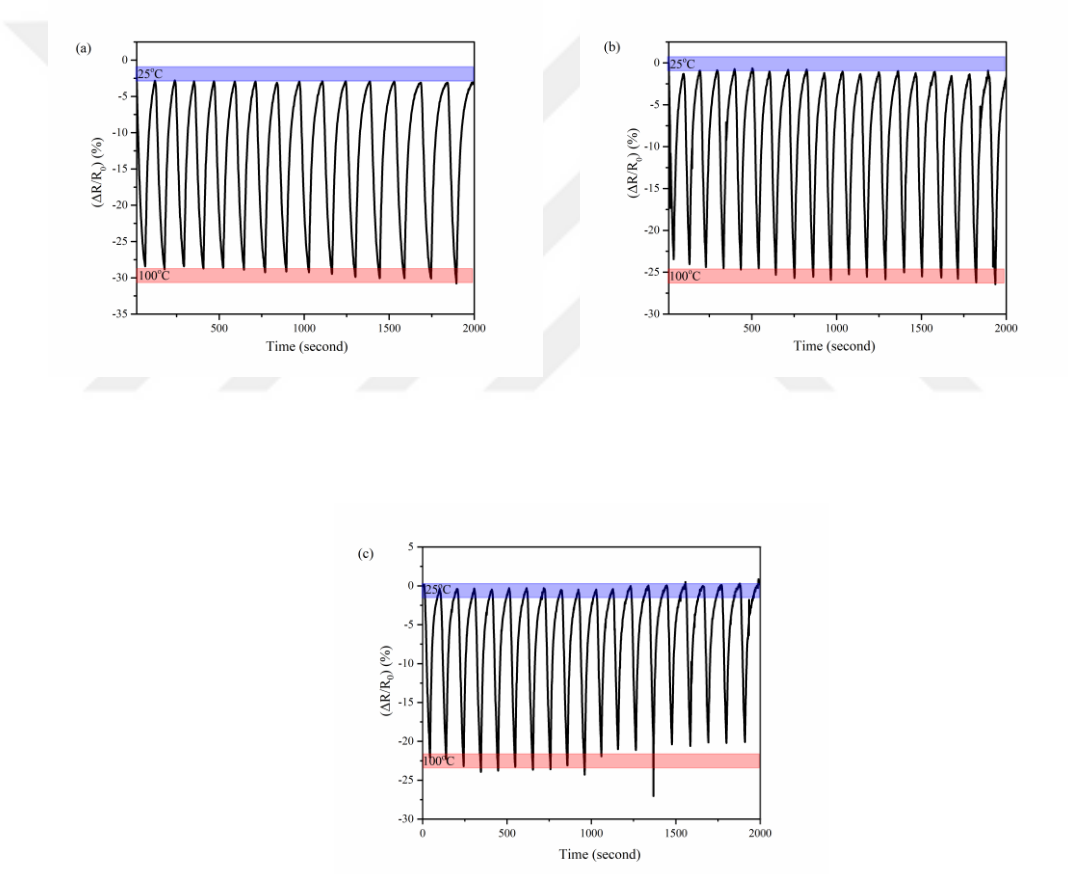

Figure 4.22 Repeatbility of (a) 20Bc, (b) 25Bc, (c) 30Bc samples on PVC substrate between 25–100 °C

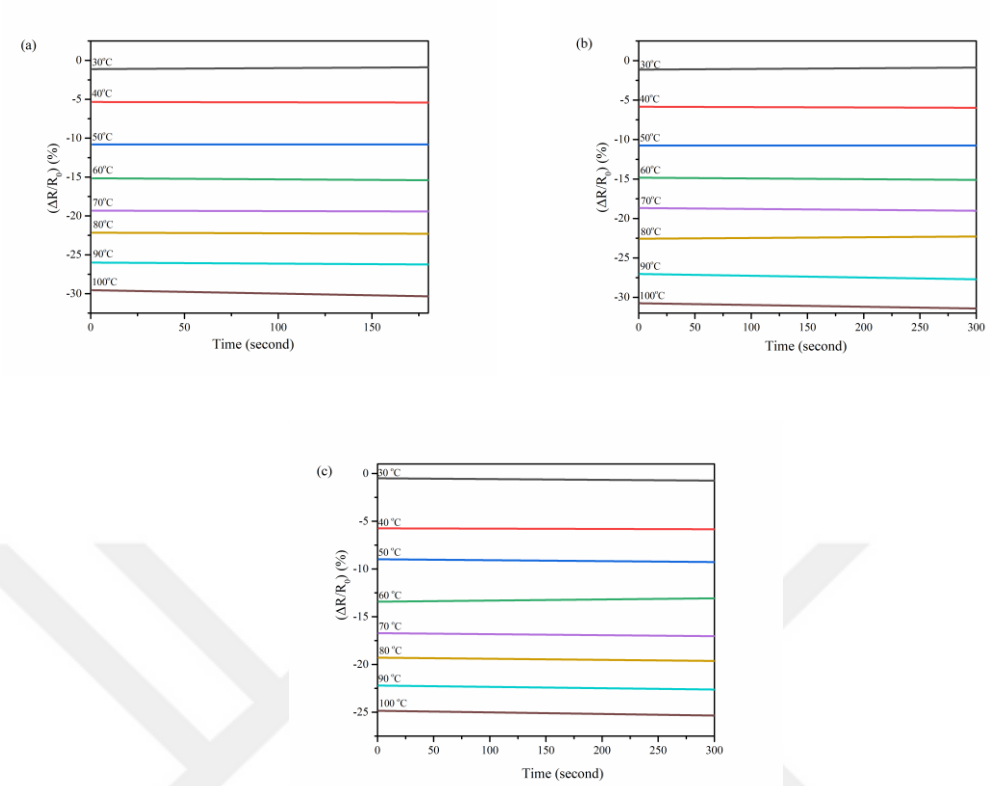

Figure 4.23 Long-term stability of (a) 20Bc, (b) 25Bc, and (c) 30Bc samples on PVC substrate between 25–100 °C

Figure 4.23 depicts the long-term stability test results for biochar-based samples on a PVC substrate. It is evident that all samples demonstrated robust stability over the specified time frame. A comparison of the performance of the biochar-based sample on glass and PVC substrates revealed that they exhibited similar results. Furthermore, in contrast to the graphite-based sample on the PVC substrate, the biochar-based samples demonstrated superior performance. This phenomenon can be related to the smaller particle size of the biochar powders. When subjected to heating and cooling conditions, the conductive particles move away from each other. The higher particle size of graphite results in an increase in the gaps between the larger particles when heated, which causes a fluctuation in resistivity. In contrast, the biochar particles with a smaller particle size than graphite and they can fill these gaps between the large particles, thereby providing a continuous conductive pathway under the same conditions. Moreover, closer contact between particles minimizes the contact resistance between adjacent particles, resulting in an improvement in electrical

conductivity (Antunes et al., 2011; Király & Ronkay, 2015). This phenomenon resulted in better performance in terms of long-term stability in biochar-based samples on PVC substrate.

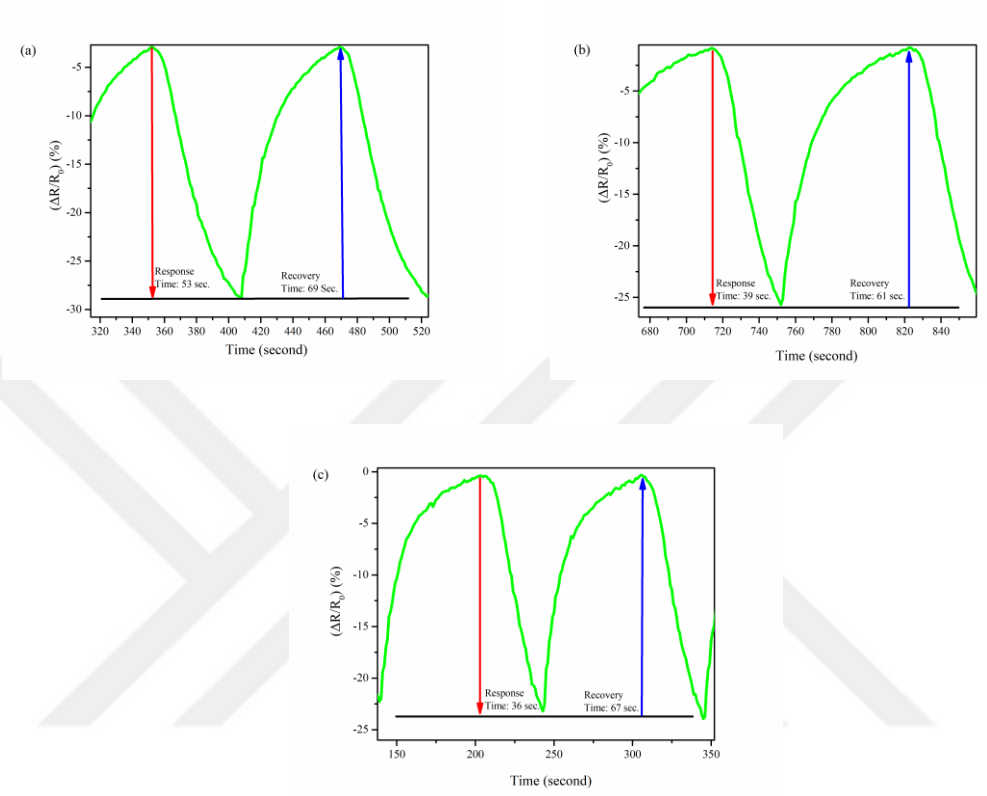

Figure 4.24 Response and recovery time of (a) 20Bc, (b) 25Bc, (c) 30Bc samples on PVC substrate between 25–100 °C

Figure 4.24 illustrates the response and recovery time of biochar-based samples on a PVC substrate. The reduction in sensor response time can be attributed to the enhanced rigidity of the samples with increasing biochar concentrations. The thermal expansion of the polymer substrate constrains this increased rigidity (Király & Ronkay, 2015). The sensors exhibited nearly similar recovery times.

In order to understand the synergistic effect of graphite and biochar, sensor experiments were conducted for hybrid composites as well (5Gr-1Bc). Figure 4.25 and Figure 4.26 show the test results of hybrid composite on glass and PVC substrate, respectively. As can be seen from the figures, the sample showed almost linear

behavior under heating and cooling conditions on a glass substrate and non-linear behavior on the PVC substrate. However, considering the fluctuation of graphite samples on PVC substrate, the combination of graphite and biochar positively affected the sensors. The addition of a small amount of biochar prevented fluctuation by filling gaps between graphite particles, reducing interparticle distance and providing a conductive path (Jing et al., 2000). Both samples exhibited good repeatability, but some resistivity changes were observed (Figure 4.25b and Figure 4.26b).

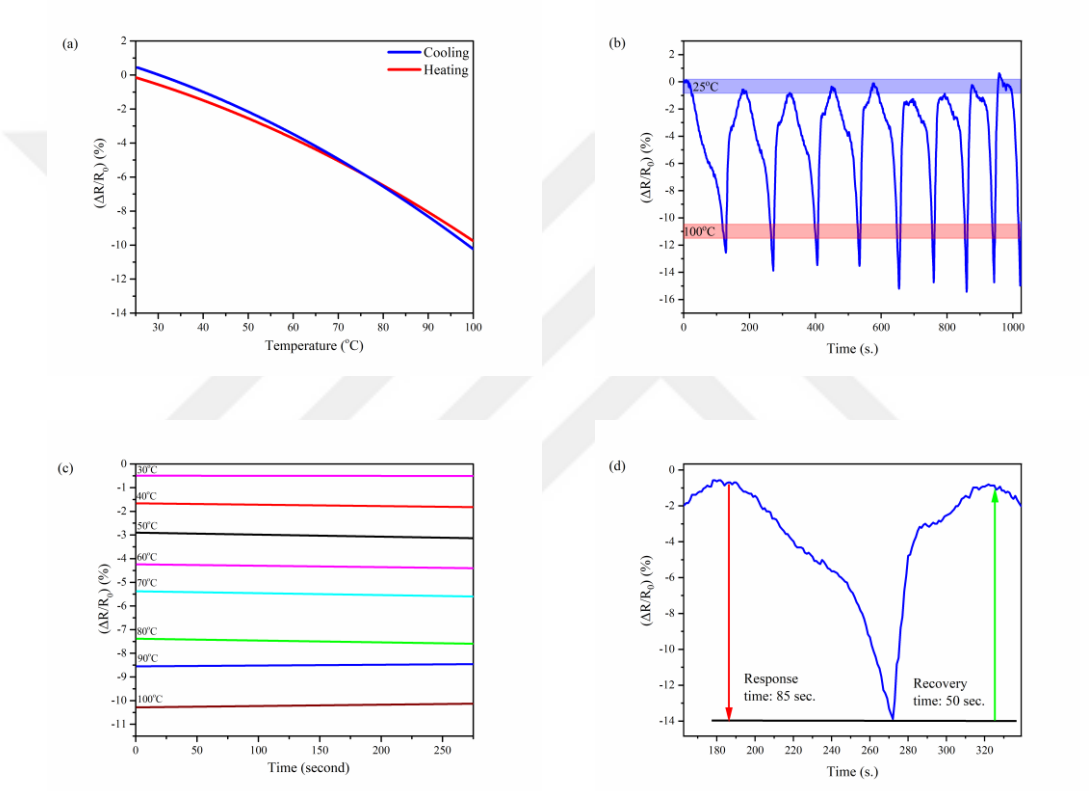

Figure 4.25 (a) Normalized response, (b) Repeatability, (c) Long-term stability, (d) Response and recovery time of hybrid composite on glass substrate between 25–100 °C

Figures 4.25c and 4.26c illustrate the long-term stability results of the samples. Both samples demonstrated favorable long-term stability characteristics. With regard to graphite-based samples on a PVC substrate, it is evident that the incorporation of biochar has a beneficial impact on the long-term stability of the samples. Conversely, the response and recovery times of the samples are illustrated in Figures 4.25d and 4.26d. As can be discerned from the figures, the samples on a glass substrate demonstrate superior response and recovery times. This phenomenon can be attributed

to the higher thermal expansion coefficient of the PVC substrate compared to the glass substrate.

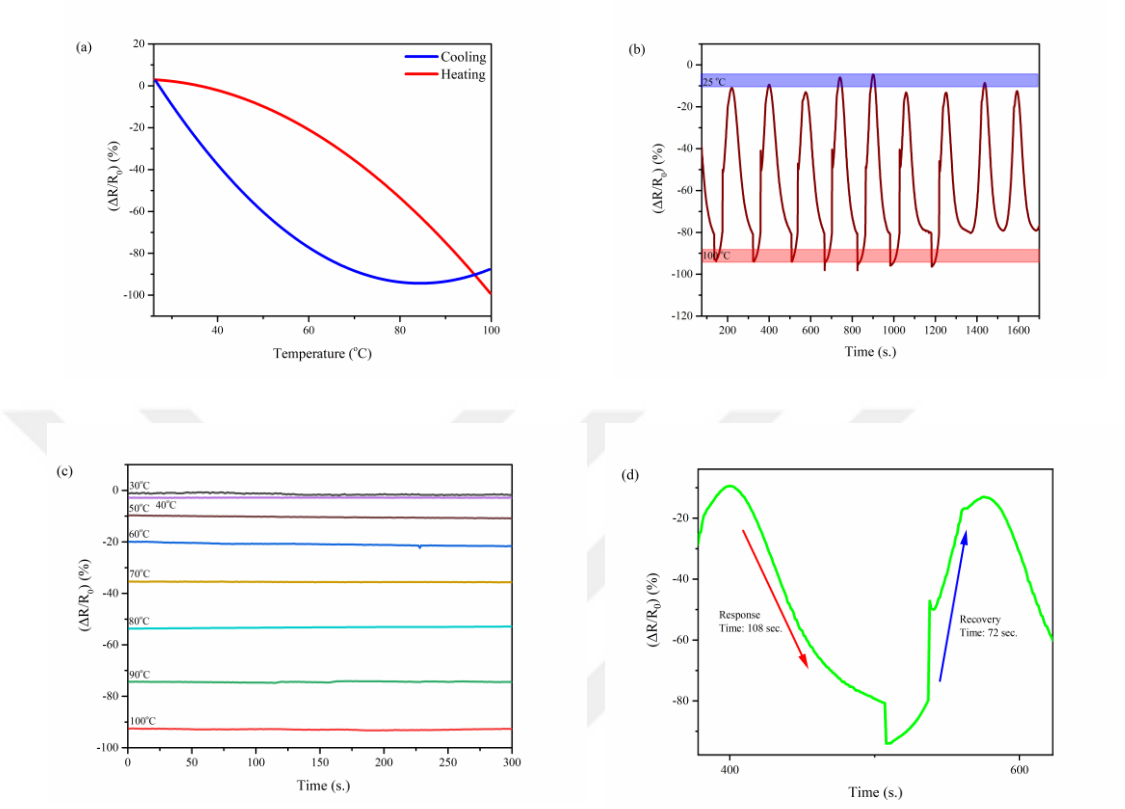

Figure 4.26 (a) Normalized response, (b) Repeatability, (c) Long-term stability, (d) Response and recovery time of hybrid composite on PVC substrate between 25–100 °C

CHAPTER FIVE
CONCLUSION

In conclusion, the utilization of graphite and biochar/SS solution composites in temperature sensor applications has been demonstrated to be effective. The findings can be summarised as follows:

1) A novel temperature-sensitive ink that has not been proposed before was successfully developed. The findings suggest that SS solution represents an appropriate matrix material for carbon-based fillers.

2) The production of biochar from waste biomass was successfully achieved. The graphite and biochar powders were blended with the SS solution in a uniform manner and subsequently applied to glass and PVC substrates using the doctor blade technique.

3) The percolation threshold of the samples was determined as 7.5 and 16.5 (wt. %) for graphite and biochar-filled composites, respectively. On the other hand, in order to understand the synergetic effect of graphite and biochar, co-percolation studies were conducted. The combination of graphite and biochar positively influenced the overall performance of the sensors and the conductivity of the composite. The new composite structure exhibited a percolation threshold of 6.5 (wt.%), as determined through analysis.

4) The sensor performance of the composites was evaluated in the range of 25-100 ℃. When graphite-based sensors were compared, sensors on glass substrate showed overall more compatible performance than samples on PVC substrate. Due to the thermal expansion of the polymer substrate and the high particle size of graphite, some fluctuations were observed in the resistivity of graphite-based samples on PVC substrate. Deterioration of the composite structure also negatively affected the long-term stability and repeatability of sensors on the PVC substrate. In general, increasing the graphite concentration had a positive effect on the overall performance of the sensors.

5) When comparing the biochar-based sensors, the sensors on PVC substrate exhibited better overall performance than the samples on glass substrate. In terms of repeatability and response and recovery time of the sensors, the samples on PVC substrate exhibited better performance than the samples on glass substrate. Increasing the biochar concentration also had a positive effect on the overall performance of the sensors.

6) Compared to graphite and biochar-based sensors, while graphite-based sensors exhibited superiority on the glass substrate, biochar-based sensors exhibited better performance on the PVC substrate. While the graphite-based sensors exhibited fluctuations on the PVC substrate, the biochar-based sensors did not show any. As mentioned before, this phenomenon is related to the expansion of the polymer substrate, the increase in resistivity, and particle sizes of graphite and biochar.

7) The synergetic effect of graphite and biochar was also investigated. The results indicated that the combination of graphite and biochar had a positive effect on the composite structure. Samples showed almost linear behavior on a glass substrate. While graphite-based sensors exhibited fluctuations on PVC substrate, the addition of only 1 wt. % biochar prevented fluctuations in resistivity. This phenomenon can be explained by filling the gaps of graphite particles with biochar particles, thus providing a continuous pathway for electron conductivity.

All in all graphite-biochar/SS solution composite coatings on glass and PVC substrates were successfully evaluated in temperature sensor applications. The results indicate that SS solution is a suitable material for carbon based materials as a matrix material in terms of ease of use and homogeneity. As a novelty, the sensors need to be encapsulated with a polymer. On the other hand, composite material is suitable for miniaturization of sensors. Miniaturization can be beneficial in terms of avoiding structural changes and improving electrical properties.

REFERENCES

Adeniyi, A. G., Iwuozor, K. O., Emenike, E. C., Amoloye, M. A., Aransiola, E. S., Motolani, F. O., & Kayode, S. H. (2023). Prospects and problems in the development of biochar-filled plastic composites: a review. In Functional Composites and Structures (Vol. 5, Issue 1, p. 012002). IOP Publishing. https://doi.org/10.1088/2631-6331/acb19b

Agbagla-Dohnani, A., Cornu, A., Nozière, P., Besle, J. M., Dulphy, J. P., Doreau, M., & Grenet, E. (2003). Microbial degradation of rice and barley straws in the sheep rumen and the donkey caecum. Journal of the Science of Food and Agriculture, 83(5), 383–394. https://doi.org/10.1002/jsfa.1386

Ain, Q. T., Haq, S. H., Alshammari, A., Al-Mutlaq, M. A., & Anjum, M. N. (2019). The systemic effect of PEG-nGO-induced oxidative stress in vivo in a rodent model. Beilstein Journal of Nanotechnology, 10, 901–911. https://doi.org/10.3762/BJNANO.10.91

Ali, S., Khan, S., & Bermak, A. (2019). Inkjet-Printed Human Body Temperature Sensor for Wearable Electronics. IEEE Access, 7, 163981–163987. https://doi.org/10.1109/ACCESS.2019.2949335

Amirov, R. K., Atamanuk, I. N., Vorobieva, N. A., Isakaev, E. H., Shavelkina, M. B., & Shkolnikov, E. I. (2015). Synthesis of graphene-like materials by pyrolysis of hydrocarbons in thermal plasma and their properties. Journal of Physics: Conference Series, 653(1), 012161. https://doi.org/10.1088/1742-6596/653/1/012161

Ando, T. (2009). The electronic properties of graphene and carbon nanotubes. In NPG Asia Materials (Vol. 1, Issue 1, pp. 17–21). Nature Publishing Group. https://doi.org/10.1038/asiamat.2009.1

Antunes, R. A., De Oliveira, M. C. L., Ett, G., & Ett, V. (2011). Carbon materials in composite bipolar plates for polymer electrolyte membrane fuel cells: A review of the main challenges to improve electrical performance. In Journal of Power Sources (Vol. 196, Issue 6, pp. 2945–2961). Elsevier.

https://doi.org/10.1016/j.jpowsour.2010.12.041

Aqel, A., El-Nour, K. M. M. A., Ammar, R. A. A., & Al-Warthan, A. (2012). Carbon nanotubes, science and technology part (I) structure, synthesis and characterisation. In Arabian Journal of Chemistry (Vol. 5, Issue 1, pp. 1–23). Elsevier. https://doi.org/10.1016/j.arabjc.2010.08.022

Arman Kuzubasoglu, B., & Kursun Bahadir, S. (2020a). Flexible temperature sensors: A review. Sensors and Actuators, A: Physical, 315. https://doi.org/10.1016/j.sna.2020.112282

Aslinezhad, M. (2020). High sensitivity refractive index and temperature sensor based on semiconductor metamaterial perfect absorber in the terahertz band. Optics Communications, 463, 125411. https://doi.org/10.1016/j.optcom.2020.125411

Bahari, S. A., & Krause, A. (2016). Utilizing Malaysian bamboo for use in thermoplastic composites. Journal of Cleaner Production, 110, 16–24. https://doi.org/10.1016/j.jclepro.2015.03.052

Bartoli, M., Troiano, M., Giudicianni, P., Amato, D., Giorcelli, M., Solimene, R., & Tagliaferro, A. (2022). Effect of heating rate and feedstock nature on electrical conductivity of biochar and biochar-based composites. Applications in Energy and Combustion Science, 12, 100089. https://doi.org/10.1016/j.jaecs.2022.100089

Besenhard, J. O. (2007). Handbook of Battery Materials. In Handbook of Battery Materials. https://doi.org/10.1002/9783527611676

Bhattacharya, S., Agarwal, A. K., Prakash, O., Singh, S., Pandey, M., & Kant, R. (2019). Introduction to Sensors for Aerospace and Automotive Applications. In Energy, Environment, and Sustainability (pp. 1–6). Springer Nature. https://doi.org/10.1007/978-981-13-3290-6_1

Brown, M. E. (2001). Introduction to thermal analysis : techniques and applications. In Thermochimica Acta (Vol. 155). Kluwer Academic Publishers.

Chae, S. J., Güneş, F., Kim, K. K., Kim, E. S., Han, G. H., Kim, S. M., Shin, H., Yoon, S. M., Choi, J. Y., Park, M. H., Yang, C. W., Pribat, D., & Lee, Y. H. (2009).

Synthesis of large-area graphene layers on poly-nickel substrate by chemical vapor deposition: Wrinkle formation. Advanced Materials, 21(22), 2328–2333. https://doi.org/10.1002/adma.200803016

Chaudhari, A. (2020). Sensing Mechanism of Hierarchical Carbon Nanocomposite Sensors and Their Applications in Structural Health Monitoring and Human Health Support. https://search.proquest.com/openview/0ffcca0996448daa45a3b3913f82f939/1?pq-origsite=gscholar&cbl=18750&diss=y

Chen, L., Xu, Z., Li, J., Li, Y., Shan, M., Wang, C., Wang, Z., Guo, Q., Liu, L., Chen, G., & Qian, X. (2012). A facile strategy to prepare functionalized graphene via intercalation, grafting and self-exfoliation of graphite oxide. Journal of Materials Chemistry, 22(27), 13460–13463. https://doi.org/10.1039/c2jm31208e

Chen, R., Das, S. R., Jeong, C., Khan, M. R., Janes, D. B., & Alam, M. A. (2013). Co-percolating graphene-wrapped silver nanowire network for high performance, highly stable, transparent conducting electrodes. Advanced Functional Materials, 23(41), 5150–5158. https://doi.org/10.1002/adfm.201300124

Chen, Z., Zhang, K. Y., Tong, X., Liu, Y., Hu, C., Liu, S., Yu, Q., Zhao, Q., & Huang, W. (2016). Phosphorescent Polymeric Thermometers for In Vitro and In Vivo Temperature Sensing with Minimized Background Interference. Advanced Functional Materials, 26(24), 4386–4396. https://doi.org/10.1002/adfm.201600706

Chiao, Y. H., Sivakumar, M., Yadav, S., Yoshikawa, S., & Hung, W. S. (2021). Eco-friendly water-based graphene/sodium silicate dispersion for electrically conductive screen-printing technique and theoretical studies. Carbon, 178, 26–36. https://doi.org/10.1016/j.carbon.2021.02.089

Childs, P. R. N. (2001). Practical Temperature Measurement. In Gastronomía ecuatoriana y turismo local. https://books.google.com/books?hl=tr&lr=&id=73Km1TpL2mkC&oi=fnd&pg=PP2&dq=Practical+Temperature+Measurement&ots=FKPk1FJTZP&sig=NBq8l7IOl4F-nrIG_-mOGj9RVgQ

Choi, S., Lee, H., Ghaffari, R., Hyeon, T., & Kim, D. H. (2016). Recent Advances in Flexible and Stretchable Bio-Electronic Devices Integrated with Nanomaterials. Advanced Materials, 28(22), 4203–4218. https://doi.org/10.1002/adma.201504150

Chukanov, N. V., & Chervonnyi, A. D. (2016). Infrared Spectroscopy of Minerals and Related Compounds. In Springer. Springer International Publishing. https://doi.org/10.1007/978-3-319-25349-7

Chung, D. D. L. (2002). Review: Graphite. In Journal of Materials Science (Vol. 37, Issue 8, pp. 1475–1489). https://doi.org/10.1023/A:1014915307738

Dai, L. (2006). Carbon nanotechnology: Recent developments in chemistry, physics, materials science and device applications. In Carbon Nanotechnology: Recent Developments in Chemistry, Physics, Materials Science and Device Applications. https://doi.org/10.1016/B978-0-444-51855-2.X5000-1

Dalmis, R., Kilic, G. B., Seki, Y., Koktas, S., & Keskin, O. Y. (2020). Characterization of a novel natural cellulosic fiber extracted from the stem of Chrysanthemum morifolium. Cellulose, 27(15), 8621–8634. https://doi.org/10.1007/s10570-020-03385-2

Dan, L., & Elias, A. L. (2020). Flexible and Stretchable Temperature Sensors Fabricated Using Solution-Processable Conductive Polymer Composites. Advanced Healthcare Materials, 9(16), 2000380. https://doi.org/10.1002/adhm.202000380

De Rosa, I. M., Kenny, J. M., Puglia, D., Santulli, C., & Sarasini, F. (2010). Morphological, thermal and mechanical characterization of okra (Abelmoschus esculentus) fibres as potential reinforcement in polymer composites. Composites Science and Technology, 70(1), 116–122. https://doi.org/10.1016/j.compscitech.2009.09.013

Dehkhoda, A. M., Ellis, N., & Gyenge, E. (2014). Electrosorption on activated biochar: Effect of thermo-chemical activation treatment on the electric double layer capacitance. Journal of Applied Electrochemistry, 44(1), 141–157. https://doi.org/10.1007/s10800-013-0616-4

Dimiev, A., & Eigler, S. (2016). Graphene oxide: fundamentals and applications. https://books.google.com/books?hl=tr&lr=&id=P1AeDQAAQBAJ&oi=fnd&pg=PR13&dq=graphene+oxide+production&ots=osH7TpZAL3&sig=gyxNavLOw1M1ILMMWc69YVV1eeY

Dong, H., Leung, A. K., Liu, J., Chen, R., & Lui, W. (2024). Microstructural investigation of the unsaturated hydraulic properties of hydrochar-amended soils. Acta Geotechnica, 19(2), 833–853. https://doi.org/10.1007/s11440-024-02254-7

Drogin, I. (1968). Carbon black. Journal of the Air Pollution Control Association, 18(4), 216–228. https://doi.org/10.1080/00022470.1968.10469118

Epp, J. (2016). X-Ray Diffraction (XRD) Techniques for Materials Characterization. In Materials Characterization Using Nondestructive Evaluation (NDE) Methods (pp. 81–124). Woodhead Publishing. https://doi.org/10.1016/B978-0-08-100040-3.00004-3

Fan, Q., Sun, J., Chu, L., Cui, L., Quan, G., Yan, J., Hussain, Q., & Iqbal, M. (2018). Effects of chemical oxidation on surface oxygen-containing functional groups and adsorption behavior of biochar. Chemosphere, 207, 33–40. https://doi.org/10.1016/j.chemosphere.2018.05.044

Ferrari, A., & Robertson, J. (2000). Interpretation of Raman spectra of disordered and amorphous carbon. Physical Review B - Condensed Matter and Materials Physics, 61(20), 14095–14107. https://doi.org/10.1103/PhysRevB.61.14095

Fraden, J. (2010). Handbook of Modern Sensors. In Handbook of Modern Sensors. Springer New York. https://doi.org/10.1007/978-1-4419-6466-3

Fukada, S., Shintani, Y., Shimomura, M., Tahara, F., & Yagi, R. (2012). Graphene made by mechanical exfoliation of graphite intercalation compound. Japanese Journal of Applied Physics, 51(8 PART 1), 085101. https://doi.org/10.1143/JJAP.51.085101

Geim, A. K., & Novoselov, K. S. (2009). The rise of graphene. In Nanoscience and Technology: A Collection of Reviews from Nature Journals (pp. 11–19).

https://doi.org/10.1142/9789814287005_0002

Geng, Y., Cao, R., Innocent, M. T., Hu, Z., Zhu, L., Wang, L., Xiang, H., & Zhu, M. (2022). A high-sensitive wearable sensor based on conductive polymer composites for body temperature monitoring. Composites Part A: Applied Science and Manufacturing, 163, 107269. https://doi.org/10.1016/j.compositesa.2022.107269

Georgakilas, V., Perman, J. A., Tucek, J., & Zboril, R. (2015). Broad Family of Carbon Nanoallotropes: Classification, Chemistry, and Applications of Fullerenes, Carbon Dots, Nanotubes, Graphene, Nanodiamonds, and Combined Superstructures. In Chemical Reviews (Vol. 115, Issue 11, pp. 4744–4822). American Chemical Society. https://doi.org/10.1021/cr500304f

Halasz, I., Agarwal, M., Li, R., & Miller, N. (2010). What can vibrational spectroscopy tell about the structure of dissolved sodium silicates? Microporous and Mesoporous Materials, 135(1–3), 74–81. https://doi.org/10.1016/j.micromeso.2010.06.013

Hammock, M. L., Chortos, A., Tee, B. C. K., Tok, J. B. H., & Bao, Z. (2013). 25th anniversary article: The evolution of electronic skin (E-Skin): A brief history, design considerations, and recent progress. Advanced Materials, 25(42), 5997–6038. https://doi.org/10.1002/adma.201302240

Huang, J., Yang, X., Her, S. C., & Liang, Y. M. (2019). Carbon nanotube/graphene nanoplatelet hybrid film as a flexible multifunctional sensor. Sensors (Switzerland), 19(2). https://doi.org/10.3390/s19020317

Husain, M. D., & Kennon, R. (2013). Preliminary investigations into the development of textile based temperature sensor for healthcare applications. Fibers, 1(1), 2–10. https://doi.org/10.3390/fib1010002

Inagaki, M., & Kang, F. (2016). Materials Science and Engineering of Carbon. In Materials Science and Engineering of Carbon. https://doi.org/10.1016/c2014-0-03769-0

Jariwala, D., Sangwan, V. K., Lauhon, L. J., Marks, T. J., & Hersam, M. C. (2013). Carbon nanomaterials for electronics, optoelectronics, photovoltaics, and sensing.

Chemical Society Reviews, 42(7), 2824–2860. https://doi.org/10.1039/c2cs35335k

Javaid, M., Haleem, A., Rab, S., Pratap Singh, R., & Suman, R. (2021). Sensors for daily life: A review. In Sensors International (Vol. 2, p. 100121). Elsevier. https://doi.org/10.1016/j.sintl.2021.100121

Javaid, M., Haleem, A., Singh, R. P., Rab, S., & Suman, R. (2021). Significance of sensors for industry 4.0: Roles, capabilities, and applications. In Sensors International (Vol. 2, p. 100110). Elsevier. https://doi.org/10.1016/j.sintl.2021.100110

Jing, X., Zhao, W., & Lan, L. (2000). Effect of particle size on electric conducting percolation threshold in polymer/conducting particle composites. Journal of Materials Science Letters, 19(5), 377–379. https://doi.org/10.1023/A:1006774318019

John, M. J., & Thomas, S. (2008). Biofibres and biocomposites. In Carbohydrate Polymers (Vol. 71, Issue 3, pp. 343–364). https://doi.org/10.1016/j.carbpol.2007.05.040

Kane, S., Ulrich, R., Harrington, A., Stadie, N. P., & Ryan, C. (2021). Physical and chemical mechanisms that influence the electrical conductivity of lignin-derived biochar. Carbon Trends, 5, 100088. https://doi.org/10.1016/j.cartre.2021.100088

Karimi, M., Solati, N., Amiri, M., Mirshekari, H., Mohamed, E., Taheri, M., Hashemkhani, M., Saeidi, A., Estiar, M. A., Kiani, P., Ghasemi, A., Basri, S. M. M., Aref, A. R., & Hamblin, M. R. (2015). Carbon nanotubes part I: Preparation of a novel and versatile drug-delivery vehicle. In Expert Opinion on Drug Delivery (Vol. 12, Issue 7, pp. 1071–1087). Informa Healthcare. https://doi.org/10.1517/17425247.2015.1003806

Karimov, K. H. S., Khalid, F. A., Tariq Saeed Chani, M., Mateen, A., Asif Hussain, M., & Maqbool, A. (2012). Carbon nanotubes based flexible temperature sensors. Optoelectronics and Advanced Materials, Rapid Communications, 6(1–2), 194–196. https://www.researchgate.net/profile/Adnan-Maqbool-2/publication/260337226_Carbon_nanotubes_based_flexible_temperature_sensor

s/links/0f317530cd18bdf90a000000/Carbon-nanotubes-based-flexible-temperature-sensors.pdf

Keskin, O. Yasin, Dalmis, R., Balci Kilic, G., Seki, Y., & Koktas, S. (2020). Extraction and characterization of cellulosic fiber from Centaurea solstitialis for composites. In Cellulose (Vol. 27, Issue 17, pp. 9963–9974). Springer Science and Business Media B.V. https://doi.org/10.1007/s10570-020-03498-8

Keskin, Ozgur Yasin, & Erol, M. (2023a). A new solution-based matrix material for temperature sensors. Journal of Materials Science: Materials in Electronics, 34(16), 1–11. https://doi.org/10.1007/s10854-023-10683-5

Keskin, Ozgur Yasin, Koktas, S., Seki, Y., Dalmis, R., Kilic, G. B., & Albayrak, D. (2024). Natural cellulosic fiber from Carex panicea stem for polymer composites: extraction and characterization. Biomass Conversion and Biorefinery, 14(13), 13901–13912. https://doi.org/10.1007/s13399-022-03458-1

Khan, S., Ali, S., Khan, A., & Bermak, A. (2023). Wearable Printed Temperature Sensors: Short Review on Latest Advances for Biomedical Applications. IEEE Reviews in Biomedical Engineering, 16, 152–170. https://doi.org/10.1109/RBME.2021.3121480

Khan, Y., Ostfeld, A. E., Lochner, C. M., Pierre, A., & Arias, A. C. (2016). Monitoring of Vital Signs with Flexible and Wearable Medical Devices. In Advanced Materials (Vol. 28, Issue 22, pp. 4373–4395). Wiley-VCH Verlag. https://doi.org/10.1002/adma.201504366

Király, A., & Ronkay, F. (2015). Temperature dependence of electrical properties in conductive polymer composites. Polymer Testing, 43, 154–162. https://doi.org/10.1016/j.polymertesting.2015.03.011

Kompan, T. A., Korenev, A. S., & Lukin, A. Y. (2008). Investigation of thermal expansion of a glass-ceramic material with an extra-low thermal linear expansion coefficient. International Journal of Thermophysics, 29(5), 1896–1905. https://doi.org/10.1007/s10765-008-0477-y

Kühner, G., & Voll, M. (2018). Manufacture of Carbon Black. In Carbon Black (pp. 1–66). Routledge. https://doi.org/10.1201/9781315138763-1

Kumar, A. (2018). Methods and Materials for Smart Manufacturing: Additive Manufacturing, Internet of Things, Flexible Sensors and Soft Robotics. Manufacturing Letters, 15, 122–125. https://doi.org/10.1016/j.mfglet.2017.12.014

Le, C. M., & Le, T. H. (2021). The Study's Chemical Interaction of the Sodium Silicate Solution with Extender Pigments to Investigate High Heat Resistance Silicate Coating. Journal of Analytical Methods in Chemistry, 2021. https://doi.org/10.1155/2021/5510193

Lead, C.-O., Folland, C. K., Lead, T. R. K., Christy, J. R., Clarke, R. A., Gruza, G. V, Jouzel, J., Mann, M. E., Oerlemans, J., Salinger, M. J., Wang, S.-W., Authors, C., Bates, J., Crowe, M., Frich, P., Groisman, P., Hurrell, J., Jones, P., Parker, D., … Zhai, P. (2001). Observed Climate Variability and Change 2 Contents. Intergovernmental Panel on Climate Change. https://hal.science/hal-03333964/

Lehmann, J., & Stephen, J. (2015). Biochar for Environmental Management: Science, Technology and Implementation. In Science And Technology (Vol. 1). https://books.google.com/books?hl=tr&lr=&id=gWDABgAAQBAJ&oi=fnd&pg=PP1&dq=Biochar+for+Environmental+Management:+Science+and+Technology.&ots=t_TnDQDVpV&sig=79vpU4DUqnMBpzXNs8paAnD2ULU

Leigh, J. (1988). Temperature measurement and control. https://books.google.com/books?hl=tr&lr=&id=SWsa_PpJzbcC&oi=fnd&pg=PR5&dq=Handbook+of+Temperature+Measurement&ots=d02Xqfc5vD&sig=O6qnWbnplYyE_8cDwLKoql4n_ZU

Li, Q., Zhang, L. N., Tao, X. M., & Ding, X. (2017). Review of Flexible Temperature Sensing Networks for Wearable Physiological Monitoring. Advanced Healthcare Materials, 6(12), 1601371. https://doi.org/10.1002/adhm.201601371

Li, Y. S., Liao, J. L., Wang, S. Y., & Chiang, W. H. (2016). Intercalation-assisted longitudinal unzipping of carbon nanotubes for green and scalable synthesis of graphene nanoribbons. Scientific Reports, 6, 22755.

https://doi.org/10.1038/srep22755

Li, Z., Wang, L., Li, Y., Feng, Y., & Feng, W. (2019). Carbon-based functional nanomaterials: Preparation, properties and applications. In Composites Science and Technology (Vol. 179, pp. 10–40). Elsevier. https://doi.org/10.1016/j.compscitech.2019.04.028

Lichtenwalner, D. J., Hydrick, A. E., & Kingon, A. I. (2007). Flexible thin film temperature and strain sensor array utilizing a novel sensing concept. Sensors and Actuators, A: Physical, 135(2), 593–597. https://doi.org/10.1016/j.sna.2006.07.019

Lin, M., Zheng, Z., Yang, L., Luo, M., Fu, L., Lin, B., & Xu, C. (2022). A High-Performance, Sensitive, Wearable Multifunctional Sensor Based on Rubber/CNT for Human Motion and Skin Temperature Detection. Advanced Materials, 34(1), 2107309. https://doi.org/10.1002/adma.202107309

Liu, D., Ma, J., Zheng, S., Shao, W., Zhang, T., Liu, S., Jian, X., Wu, Z., & Hu, F. (2023). High-Performance and Flexible Co-Planar Integrated Microsystem of Carbon-Based All-Solid-State Micro-Supercapacitor and Real-Time Temperature Sensor. Energy and Environmental Materials, 6(6), e12445. https://doi.org/10.1002/eem2.12445

Liu, G., Tan, Q., Kou, H., Zhang, L., Wang, J., Lv, W., Dong, H., & Xiong, J. (2018). A flexible temperature sensor based on reduced graphene oxide for robot skin used in internet of things. Sensors (Switzerland), 18(5), 1400. https://doi.org/10.3390/s18051400

Liu, Q., Tai, H., Yuan, Z., Zhou, Y., Su, Y., Jiang, Y., Liu, Q., Tai, H., Yuan, Z., Zhou, Y., Su, Y., & Jiang, Y. (2019). A High-Performances Flexible Temperature Sensor Composed of Polyethyleneimine/Reduced Graphene Oxide Bilayer for Real-Time Monitoring. Advanced Materials Technologies, 4(3), 1800594. https://doi.org/10.1002/ADMT.201800594

Liu, S., Peng, S., Zhang, B., Xue, B., Yang, Z., Wang, S., & Xu, G. (2022). Effects of biochar pyrolysis temperature on thermal properties of polyethylene glycol/biochar composites as shape-stable biocomposite phase change materials. RSC Advances,

12(16), 9587–9598. https://doi.org/10.1039/d1ra09167k

Long, C. M., Nascarella, M. A., & Valberg, P. A. (2013). Carbon black vs. black carbon and other airborne materials containing elemental carbon: Physical and chemical distinctions. In Environmental Pollution (Vol. 181, pp. 271–286). Elsevier. https://doi.org/10.1016/j.envpol.2013.06.009

Macklen, E. D. (1991). NTC Thermistor Materials. Concise Encyclopedia of Advanced Ceramic Materials, 328–331. https://doi.org/10.1016/B978-0-08-034720-2.50091-5

Mahmoud, W. E., & Al-Bluwi, S. A. (2020). Development of highly sensitive temperature sensor made of graphene monolayers doped P(VDF-TrFE) nanocomposites. Sensors and Actuators, A: Physical, 312, 112101. https://doi.org/10.1016/j.sna.2020.112101

Malhotra, B. D., Srivastava, S., & Augustine, S. (2015). Biosensors for food toxin detection: Carbon nanotubes and graphene. Materials Research Society Symposium Proceedings, 1725, 33–43. https://doi.org/10.1557/opl.2015.165

Malode, S. J., Shanbhag, M. M., Kumari, R., Dkhar, D. S., Chandra, P., & Shetti, N. P. (2023). Biomass-derived carbon nanomaterials for sensor applications. Journal of Pharmaceutical and Biomedical Analysis, 222, 115102. https://doi.org/10.1016/J.JPBA.2022.115102

Mathur, R. B. (2016). Carbon nanomaterials: Synthesis, structure, properties and applications. In Carbon Nanomaterials: Synthesis, Structure, Properties and Applications. CRC Press. https://doi.org/10.1201/9781315371849/CARBON-NANOMATERIALS-RAKESH-BEHARI-MATHUR-BHANU-PRATAP-SINGH-SHAILAJA-PANDE

Matinfar, M., & Nychka, J. A. (2023). A review of sodium silicate solutions: Structure, gelation, and syneresis. In Advances in Colloid and Interface Science (Vol. 322, p. 103036). Elsevier. https://doi.org/10.1016/j.cis.2023.103036

Matthias Nau. (2002). Electrical Temperature Measurement. Juchheim.

McLachlan, D. S., Blaszkiewicz, M., & Newnham, R. E. (1990). Electrical Resistivity of Composites. Journal of the American Ceramic Society, 73(8), 2187–2203. https://doi.org/10.1111/J.1151-2916.1990.TB07576.X

Megha, R., Ali, F. A., Ravikiran, Y. T., Ramana, C. H. V. V., Kiran Kumar, A. B. V., Mishra, D. K., Vijayakumari, S. C., & Kim, D. (2018). Conducting polymer nanocomposite based temperature sensors: A review. In Inorganic Chemistry Communications (Vol. 98, pp. 11–28). Elsevier. https://doi.org/10.1016/j.inoche.2018.09.040

Meijer, G., Pertijs, M., & Makinwa, K. (2014). Smart Sensor Systems: Emerging Technologies and Applications. In Smart Sensor Systems: Emerging Technologies and Applications (Vol. 9780470686). https://doi.org/10.1002/9781118701508

Michalski, L. (2001). Temperature Measurement. In Temperature Measurement. https://doi.org/10.1016/j.mpaic.2021.01.015

Mohammad, H., Stepashkin, A. A., & Tcherdyntsev, V. V. (2022). Effect of Graphite Filler Type on the Thermal Conductivity and Mechanical Behavior of Polysulfone-Based Composites. Polymers, 14(3), 399. https://doi.org/10.3390/polym14030399

Mohd Radzuan, N. A., Sulong, A. B., & Sahari, J. (2017). A review of electrical conductivity models for conductive polymer composite. International Journal of Hydrogen Energy, 42(14), 9262–9273. https://doi.org/10.1016/j.ijhydene.2016.03.045

Morterra, C., & Low, M. J. D. (1973). Reactive Silica: Novel Aspects of the Chemistry of Silica Surfaces. Annals of the New York Academy of Sciences, 220(4), 133–244. https://doi.org/10.1111/j.1749-6632.1973.tb40251.x

Nag, A., Simorangkir, R. B. V. ., Gawade, D. R., Nuthalapati, S., Buckley, J. L., O'Flynn, B., Altinsoy, M. E., & Mukhopadhyay, S. C. (2022a). Graphene-Based Wearable Temperature Sensors: A Review. Nanomaterials, 221. https://doi.org/10.3390/nano13162339

Nagata, K., Iwabuki, H., & Nigo, H. (1998). Effect of particle size of graphites on

electrical conductivity of graphite/polymer composite. Composite Interfaces, 6(5), 483–495. https://doi.org/10.1163/156855499X00161

Neitzert, H. C., Vertuccio, L., & Sorrentino, A. (2011). Epoxy/MWCNT composite as temperature sensor and Electrical heating element. IEEE Transactions on Nanotechnology, 10(4), 688–693. https://doi.org/10.1109/TNANO.2010.2068307

Obi Reddy, K., Guduri, B. R., & Rajulu, A. V. (2009). Structural characterization and tensile properties of Borassus fruit fibers. Journal of Applied Polymer Science, 114(1), 603–611. https://doi.org/10.1002/app.30584

Oh, S. Y., Dong, I. Y., Shin, Y., Hwan, C. K., Hak, Y. K., Yong, S. C., Won, H. P., & Ji, H. Y. (2005). Crystalline structure analysis of cellulose treated with sodium hydroxide and carbon dioxide by means of X-ray diffraction and FTIR spectroscopy. Carbohydrate Research, 340(15), 2376–2391. https://doi.org/10.1016/j.carres.2005.08.007

Owusu, Y. A. (1982). Physical-chemistry study of sodium silicate as a foundry sand binder. Advances in Colloid and Interface Science, 18(1–2), 57–91. https://doi.org/10.1016/0001-8686(82)85031-8

Özmihçi, F. Ö., & Balköse, D. (2013). Effects of particle size and electrical resistivity of filler on mechanical, electrical, and thermal properties of linear low density polyethylene-zinc oxide composites. Journal of Applied Polymer Science, 130(4), 2734–2743. https://doi.org/10.1002/app.39433

Papageorgiou, D. G., Kinloch, I. A., & Young, R. J. (2017). Mechanical properties of graphene and graphene-based nanocomposites. In Progress in Materials Science (Vol. 90, pp. 75–127). Pergamon. https://doi.org/10.1016/j.pmatsci.2017.07.004

Parvez, K., Yang, S., Feng, X., & Müllen, K. (2015). Exfoliation of graphene via wet chemical routes. Synthetic Metals, 210, 123–132. https://doi.org/10.1016/j.synthmet.2015.07.014

Pei, S., & Cheng, H. M. (2012). The reduction of graphene oxide. Carbon, 50(9), 3210–3228. https://doi.org/10.1016/j.carbon.2011.11.010

Peigney, A., Laurent, C., Flahaut, E., Bacsa, R. R., & Rousset, A. (2001). Specific surface area of carbon nanotubes and bundles of carbon nanotubes. Carbon, 39(4), 507–514. https://doi.org/10.1016/S0008-6223(00)00155-X

Petousis, M., Maravelakis, E., Kalderis, D., Saltas, V., Mountakis, N., Spiridaki, M., Bolanakis, N., Argyros, A., Papadakis, V., Michailidis, N., & Vidakis, N. (2024). Biochar for sustainable additive manufacturing: Thermal, mechanical, electrical, and rheological responses of polypropylene-biochar composites. Biomass and Bioenergy, 186, 107272. https://doi.org/10.1016/j.biombioe.2024.107272

Phadkule, S. S., & Sarma, S. (2023a). Progress in nanocomposite based flexible temperature sensors: A review. In Measurement: Sensors (Vol. 27). https://doi.org/10.1016/j.measen.2023.100692

Qin, C., Wang, H., Yuan, X., Xiong, T., Zhang, J., & Zhang, J. (2020). Understanding structure-performance correlation of biochar materials in environmental remediation and electrochemical devices. In Chemical Engineering Journal (Vol. 382, p. 122977). Elsevier. https://doi.org/10.1016/j.cej.2019.122977

Rahman, M. T., Cheng, C. Y., Karagoz, B., Renn, M., Schrandt, M., Gellman, A., & Panat, R. (2019). High Performance Flexible Temperature Sensors via Nanoparticle Printing. ACS Applied Nano Materials, 2(5), 3280–3291. https://doi.org/10.1021/acsanm.9b00628

Rajanna, K., Nayak, M. M. (2004). Temperature Sensors. In Survey of Instrumentation and Measurement. Wiley. https://doi.org/10.1016/B978-075067729-5/50060-4

Rajendran, S., Palani, G., Arunprasath, K., Shanmugam, V., Marimuthu, U., & Veerasimman, A. (2024). Eco-friendly sugarcane biochar filler for enhanced mechanical properties in S-glass/polyester hybrid composites. Cleaner Engineering and Technology, 20, 100759. https://doi.org/10.1016/j.clet.2024.100759

Rajendran, S., Palani, G., Shanmugam, V., Kanagaraj, A., Veerasimman, A., & Marimuthu, U. (2024). Comparative analysis of mechanical and erosion performance of cashew and sugarcane waste based biochar-reinforced polyester composites. Cleaner Engineering and Technology, 18, 100718.

https://doi.org/10.1016/j.clet.2023.100718

Rajendran, S., Palani, G., Veerasimman, A., Marimuthu, U., Kannan, K., & Shanmugam, V. (2024). Biochar from cashew nut shells: A sustainable reinforcement for enhanced mechanical performance in hemp fibre composites. Cleaner Engineering and Technology, 20, 100745. https://doi.org/10.1016/j.clet.2024.100745

Rao, C. N. R., Biswas, K., Subrahmanyam, K. S., & Govindaraj, A. (2009). Graphene, the new nanocarbon. Journal of Materials Chemistry, 19(17), 2457–2469. https://doi.org/10.1039/b815239j

Ravindra, N., Jariwala, B., Bañobre, A., & Maske, A. (2018). Thermoelectrics: fundamentals, materials selection, properties, and performance. https://books.google.com/books?hl=tr&lr=&id=hBxrDwAAQBAJ&oi=fnd&pg=PR5&dq=Thermoelectrics_+Fundamentals,+Materials+Selection,+Properties,+and+Performance&ots=ygzZaDjMJt&sig=cG6s7k02xo_5GRWzRtzLtNcjL-w

Rew, Y., Baranikumar, A., Tamashausky, A. V., El-Tawil, S., & Park, P. (2017). Electrical and mechanical properties of asphaltic composites containing carbon based fillers. Construction and Building Materials, 135, 394–404. https://doi.org/10.1016/j.conbuildmat.2016.12.221

Ribeiro, B., Botelho, E. C., Costa, M. L., & Bandeira, C. F. (2017). Carbon nanotube buckypaper reinforced polymer composites: A review. In Polimeros (Vol. 27, Issue 3, pp. 247–255). Associação Brasileira de Polímeros. https://doi.org/10.1590/0104-1428.03916

Ridzuan, M. J. M., Abdul Majid, M. S., Afendi, M., Aqmariah Kanafiah, S. N., Zahri, J. M., & Gibson, A. G. (2016). Characterisation of natural cellulosic fibre from Pennisetum purpureum stem as potential reinforcement of polymer composites. Materials and Design, 89, 839–847. https://doi.org/10.1016/j.matdes.2015.10.052

Saba, N., Jawaid, M., Fouad, H., Its, O. A.-N. and, & 2019, U. (2019). Nanocarbon: Preparation, properties, and applications. In Elsevier (pp. 327–354). https://www.sciencedirect.com/science/article/pii/B9780081025093000092

Saravanakumar, S. S., Kumaravel, A., Nagarajan, T., Sudhakar, P., & Baskaran, R. (2013). Characterization of a novel natural cellulosic fiber from Prosopis juliflora bark. Carbohydrate Polymers, 92(2), 1928–1933. https://doi.org/10.1016/j.carbpol.2012.11.064

Shen, C. hui, Mu, P., & Yuan, R. zhang. (2006). Sodium silicate/graphite conductive composite bipolar plates for proton exchange membrane fuel cells. Journal of Power Sources, 162(1), 460–463. https://doi.org/10.1016/j.jpowsour.2006.06.095

Shih, W. P., Tsao, L. C., Lee, C. W., Cheng, M. Y., Chang, C., Yang, Y. J., & Fan, K. C. (2010). Flexible temperature sensor array based on a Graphite-Polydimethylsiloxane composite. Sensors, 10(4), 3597–3610. https://doi.org/10.3390/s100403597

Siburian, R., Sihotang, H., Lumban Raja, S., Supeno, M., & Simanjuntak, C. (2018). New route to synthesize of graphene nano sheets. Oriental Journal of Chemistry, 34(1), 182–187. https://doi.org/10.13005/ojc/340120

Soni, M., Bhattacharjee, M., Ntagios, M., & Dahiya, R. (2020). Printed Temperature Sensor Based on PEDOT: PSS-Graphene Oxide Composite. IEEE Sensors Journal, 20(14), 7525–7531. https://doi.org/10.1109/JSEN.2020.2969667

Su, K., Tian, X., Li, Z., & Liu, X. (2023). Oxidation behavior of Ti3SiC2 powder synthesized by using biochar, Si and Ti. Ceramics International, 49(3), 4863–4871. https://doi.org/10.1016/j.ceramint.2022.09.377

Su, Y., Ma, C., Chen, J., Wu, H., Luo, W., Peng, Y., Luo, Z., Li, L., Tan, Y., Omisore, O. M., Zhu, Z., Wang, L., & Li, H. (2020). Printable, Highly Sensitive Flexible Temperature Sensors for Human Body Temperature Monitoring: A Review. In Nanoscale Research Letters (Vol. 15, Issue 1, pp. 1–34). Springer. https://doi.org/10.1186/s11671-020-03428-4

Takei, K., Honda, W., Harada, S., Arie, T., & Akita, S. (2015). Toward flexible and wearable human-interactive health-monitoring devices. Advanced Healthcare Materials, 4(4), 487–500. https://doi.org/10.1002/adhm.201400546

Tarani, E., Arvanitidis, I., Christofilos, D., Bikiaris, D. N., Chrissafis, K., & Vourlias, G. (2023). Calculation of the degree of crystallinity of HDPE/GNPs nanocomposites by using various experimental techniques: a comparative study. Journal of Materials Science, 58(4), 1621–1639. https://doi.org/10.1007/s10853-022-08125-4

Tetlow, H., Posthuma de Boer, J., Ford, I. J., Vvedensky, D. D., Coraux, J., & Kantorovich, L. (2014). Growth of epitaxial graphene: Theory and experiment. In Physics Reports (Vol. 542, Issue 3, pp. 195–295). North-Holland. https://doi.org/10.1016/j.physrep.2014.03.003

Tiwari, S. K., Bystrzejewski, M., De Adhikari, A., Huczko, A., & Wang, N. (2022). Methods for the conversion of biomass waste into value-added carbon nanomaterials: Recent progress and applications. Progress in Energy and Combustion Science, 92, 101023. https://doi.org/10.1016/J.PECS.2022.101023

Tonkov, D. N., Kobylyatskaya, M. I., Vasilyeva, E. S., Semencha, A. V., & Gasumyants, V. E. (2022). Conductive properties of flexible polymer composites with different carbon-based fillers. Journal of Physics: Conference Series, 2227(1). https://doi.org/10.1088/1742-6596/2227/1/012022

Trung, T. Q., Ramasundaram, S., Hwang, B. U., & Lee, N. E. (2016). An All-Elastomeric Transparent and Stretchable Temperature Sensor for Body-Attachable Wearable Electronics. Advanced Materials, 28(3), 502–509. https://doi.org/10.1002/adma.201504441

Turkani, V. S., Maddipatla, D., Narakathu, B. B., Bazuin, B. J., & Atashbar, M. Z. (2018). A carbon nanotube based NTC thermistor using additive print manufacturing processes. Sensors and Actuators, A: Physical, 279, 1–9. https://doi.org/10.1016/j.sna.2018.05.042

Uddin, M. N., Rahman, M. M., & Asmatulu, R. (2017). Recent Progress on Synthesis, Characterization and Applications of Carbon Black Nanoparticles. In Advances in Nanotechnology (Vol. 19, pp. 40–78). https://www.researchgate.net/profile/Md-Uddin-

74/publication/319035010_Recent_Progress_on_Synthesis_Characterization_and_Applications_of_Carbon_Black_Nanoparticles/links/598bc496a6fdcc58acb3ab5f/Recent-Progress-on-Synthesis-Characterization-and-Applicatio

Ul-Hamid, A. (2018). A Beginners' Guide to Scanning Electron Microscopy: Questions & answers. In SPRINGER (Vol. 9, Issue 27 Suppl Nu).

Uma Maheswari, C., Obi Reddy, K., Muzenda, E., Guduri, B. R., & Varada Rajulu, A. (2012). Extraction and characterization of cellulose microfibrils from agricultural residue - Cocos nucifera L. Biomass and Bioenergy, 46, 555–563. https://doi.org/10.1016/j.biombioe.2012.06.039

Velmurugan G, Chohan, J. S., Manikandan T, Gururama Senthilvel P, John Presin Kumar A, Nagaraj M, Mohan Raj N, & Nagalakshmi, T. J. (2024). Evaluation of mechanical, thermal, and flammability properties in biochar-infused polymer composites from bael fruit and cashew shells: a comparative study. Biomass Conversion and Biorefinery, 1–17. https://doi.org/10.1007/s13399-024-06020-3

Verma, A., Bandyopadhyay, R., Tiwary, C. S., Kanti Das, B., & Bhattacharya, J. (2023). Engineering defect concentration and morphology of green graphene for the development of hard and anticorrosive coating on carbon steel. Corrosion Science, 224, 111523. https://doi.org/10.1016/j.corsci.2023.111523

Vetelino, J. F., & Reghu, A. (2017). Introduction to sensors. In Introduction to Sensors. https://doi.org/10.1201/9781315218274

Vieira, L. de S., dos Anjos, E. G. R., Verginio, G. E. A., Oyama, I. C., Braga, N. F., da Silva, T. F., Montagna, L. S., & Passador, F. R. (2022). A review concerning the main factors that interfere in the electrical percolation threshold content of polymeric antistatic packaging with carbon fillers as antistatic agent. Nano Select, 3(2), 248–260. https://doi.org/10.1002/nano.202100073

Wang, B., Yi, X., Pan, Y., & Shan, H. (1997). Volume expansion dependence of ptc effect of carbon black loaded polymer composite. Journal of Materials Science Letters, 16(24), 2005–2007. https://doi.org/10.1023/A:1018536011826

Wang, C., Xia, K., Wang, H., Liang, X., Yin, Z., & Zhang, Y. (2019). Advanced Carbon for Flexible and Wearable Electronics. In Advanced Materials (Vol. 31, Issue 9, p. 1801072). John Wiley & Sons, Ltd. https://doi.org/10.1002/adma.201801072

Wang, L., Zhang, Q., Chen, S., Xu, F., Chen, S., Jia, J., Tan, H., Hou, H., & Song, Y. (2014). Electrochemical sensing and biosensing platform based on biomass-derived macroporous carbon materials. Analytical Chemistry, 86(3), 1414–1421. https://doi.org/10.1021/AC401563M/SUPPL_FILE/AC401563M_SI_001.PDF

Wang, N., Sun, H., Yang, X., Lin, W., He, W., Liu, H., Bhat, G., & Yu, B. (2022a). Flexible temperature sensor based on RGO/CNTs@PBT melting blown nonwoven fabric. Sensors and Actuators A: Physical, 339. https://doi.org/10.1016/j.sna.2022.113519

Wang, Q., Yu, Y., Yang, J., & Liu, J. (2015). Fast Fabrication of Flexible Functional Circuits Based on Liquid Metal Dual-Trans Printing. Advanced Materials, 27(44), 7109–7116. https://doi.org/10.1002/adma.201502200

Wang, Y., Yang, B., Hua, Z., Zhang, J., Guo, P., Hao, D., Gao, Y., & Huang, J. (2022). Recent advancements in flexible and wearable sensors for biomedical and healthcare applications. Journal of Physics D: Applied Physics, 55(13), 134001. https://doi.org/10.1088/1361-6463/ac3c73

Webster, J. G., & Eren, H. (2018). Measurement, Instrumentation, and Sensors Handbook. In Measurement, Instrumentation, and Sensors Handbook. CRC Press. https://doi.org/10.1201/9781315217109

Wu, L., Qian, J., Peng, J., Wang, K., Liu, Z., Ma, T., Zhou, Y., Wang, G., & Ye, S. (2019). Screen-printed flexible temperature sensor based on FG/CNT/PDMS composite with constant TCR. Journal of Materials Science: Materials in Electronics, 30(10), 9593–9601. https://doi.org/10.1007/s10854-019-01293-1

Xiao, Y., Jiang, S., Li, Y., & Zhang, W. (2021). Screen-printed flexible negative temperature coefficient temperature sensor based on polyvinyl chloride/carbon black composites. Smart Materials and Structures, 30(2), 025035.

https://doi.org/10.1088/1361-665X/abd83a

Xue, Q. (2004). The influence of particle shape and size on electric conductivity of metal-polymer composites. European Polymer Journal, 40(2), 323–327. https://doi.org/10.1016/j.eurpolymj.2003.10.011

Yan, Y., Manickam, S., Lester, E., Wu, T., & Pang, C. H. (2021). Synthesis of graphene oxide and graphene quantum dots from miscanthus via ultrasound-assisted mechano-chemical cracking method. Ultrasonics Sonochemistry, 73, 105519. https://doi.org/10.1016/j.ultsonch.2021.105519

Yang, X., Zhu, W., & Yang, Q. (2008). The Viscosity Properties of Sodium Silicate Solutions. Journal of Solution Chemistry, 37, 73–83. https://doi.org/https://doi.org/10.1007/s10953-007-9214-6

Yang, J., Wei, D., Tang, L., Song, X., Luo, W., Chu, J., Gao, T., Shi, H., & Du, C. (2015). Wearable temperature sensor based on graphene nanowalls. RSC Advances, 5(32), 25609–25615. https://doi.org/10.1039/c5ra00871a

Yee, M. J., Mubarak, N. M., Abdullah, E. C., Khalid, M., Walvekar, R., Karri, R. R., Nizamuddin, S., & Numan, A. (2019). Carbon nanomaterials based films for strain sensing application—A review. In Nano-Structures and Nano-Objects (Vol. 18, p. 100312). Elsevier. https://doi.org/10.1016/j.nanoso.2019.100312

Yokotaa, T., Inouea, Y., Terakawaa, Y., Reedera, J., Kaltenbrunnera, M., Wared, T., Yange, K., Mabuchif, K., Murakawag, T., Sekinoa, M., Voitc, W., Sekitania, T., & Someyaa, T. (2015). Ultraflexible, large-area, physiological temperature sensors for multipoint measurements. Proceedings of the National Academy of Sciences of the United States of America, 112(47), 14533–14538. https://doi.org/10.1073/pnas.1515650112

Yoon, S., Sim, J. K., & Cho, Y. H. (2016). A Flexible and Wearable Human Stress Monitoring Patch. Scientific Reports, 6(1), 1–11. https://doi.org/10.1038/srep23468

Yu, Q., Wei, L., Yang, X., Wang, C., Chen, J., Du, H., Shen, W., Kang, F., & Huang,

Z. H. (2022). Electrochemical synthesis of graphene oxide from graphite flakes exfoliated at room temperature. Applied Surface Science, 598, 153788. https://doi.org/10.1016/j.apsusc.2022.153788

Yurddaskal, M., Erol, M., & Celik, E. (2017). Carbon black and graphite filled conducting nanocomposite films for temperature sensor applications. Journal of Materials Science: Materials in Electronics, 28(13), 9514–9518. https://doi.org/10.1007/S10854-017-6695-Y/TABLES/2

Zhu, C., Chortos, A., Wang, Y., Pfattner, R., Lei, T., Hinckley, A. C., Pochorovski, I., Yan, X., To, J. W. F., Oh, J. Y., Tok, J. B. H., Bao, Z., & Murmann, B. (2018). Stretchable temperature-sensing circuits with strain suppression based on carbon nanotube transistors. Nature Electronics, 1(3), 183–190. https://doi.org/10.1038/s41928-018-0041-0

Zhu, G., Wang, F., Chen, L., Wang, C., Xu, Y., Chen, J., Chang, X., & Zhu, Y. (2022). Highly flexible TPU/SWCNTs composite-based temperature sensors with linear negative temperature coefficient effect and photo-thermal effect. Composites Science and Technology, 217, 109133. https://doi.org/10.1016/j.compscitech.2021.109133